# Mathematical Modelling of Bacterial Attachment to Surfaces: Biofilm Initiation

by

Fadoua El Moustaid


*Thesis presented in partial fulfilment of the requirements for the degree of Master of Science at Stellenbosch University*

The African Institute for Mathematical Sciences,
University of Stellenbosch,
6-8 Melrose Rd, Muizenberg 7945, South Africa.

Supervisor: Dr. A. Ouhinou and Dr. L. Uys

September 2011

# Declaration

By submitting this thesis electronically, I declare that the entirety of the work contained therein is my own, original work, that I am the owner of the copyright thereof (unless to the extent explicitly otherwise stated) and that I have not previously in its entirety or in part submitted it for obtaining any qualification.

Signature: .....
F. El Moustaid

Date: 2011/09/30 .....

# Abstract

Biofilms are aggregations of bacteria that can thrive wherever there is a water-surface or water-interface. Sometimes they can be beneficial; for example, biofilms are used in water and waste-water treatment. The filter used to remove contaminants acts as a scaffold for microbial attachment and growth. However, biofilms could have bad effects, especially on a persons health. They can cause chronic diseases and serious infections. The importance of biofilms in industrial and medical settings, is the main reason of the mathematical studies performed up to now, concerning biofilms.

Biofilms have been mathematical modelling targets over the last 30 years. The complex structure and growth of biofilms make them difficult to study. Biofilm formation is a multi-stage process and occurs in even the most unlikely of environmental conditions. Models of biofilms vary from the discrete to the continuous; accounting for one-species to multi-species and from one-scale to multi-scale models. A model may even have both discrete and continuous parts. The implication of these differences is that the tools used to model biofilms differ; we present and review some of these models.

The aim in this thesis is to model the early initiation of biofilm formation. This stage involves bacterial movement towards a surface and the attachment to the boundary which seeds a biofilm. We use a diffusion equation to describe a bacterial random walk and appropriate boundary conditions to model surface attachment. An analytical solution is obtained which gives the bacterial density as a function of position and time. The model is also analysed for stability. Independent of this model, we also give a reaction diffusion equation for the distribution of sensing molecules, accounting for production by the bacteria and natural degradation.

The last model we present is of Keller-Segel type, which couples the dynamics of bacterial movement to that of the sensing molecules. In this case, bacteria perform a biased random walk towards the sensing molecules. The most important part of this chapter is the derivation of the boundary conditions. The adhesion of bacteria to a surface is presented by zero-Dirichlet boundary conditions, while the equation describing sensing molecules at the interface needed particular conditions to be set. Bacteria at the boundary also produce sensing molecules, which may then diffuse and degrade. In order to obtain an equation that includes all these features we assumed that mass is

conserved. We conclude with a numerical simulation.

# Uittreksel

Biofilms is die samedromming van bakterieë wat kan floreer waar daar 'n wateroppervlakte of watertussenvlak is. Soms kan hulle voordelig wees, soos byvoorbeeld, biofilms word gebruik in water en afvalwater behandeling. Die filter wat gebruik word om smetstowwe te verwyder, dien as 'n steier vir mikrobiese verbinding en groei. Biofilms kan ook egter slegte gevolge hë, veral op 'n persoon se gesondheid. Hulle kan slepende siektes en ernstige infeksies veroorsaak. Die belangrikheid van biofilms in industriële en mediese omgewings, is die hoof rede vir die wiskundige studies wat tot dusver uitgevoer is met betrekking tot biofilms.

Biofilms is oor die afgelope 30 jaar al 'n teiken vir wiskundige modellering. Die komplekse struktuur en groei van biofilms maak dit moeilik om hul te bestudeer. Biofilm formasie is 'n multi-fase proses, en gebeur selfs in die mees onwaarskynlikste omgewings. Modelle wat biofilms beskryf wissel van die diskreet tot die kontinu, inkorporeer een of meer spesies, en strek van een- tot multi-skaal modelle. 'n Model kan ook oor beide diskreet en kontinue komponente besit. Dit beteken dat die tegnieke wat gebruik word om biofilms te modelleer ook verskil. In hierdie proefskrif verskaf ons 'n oorsig van sommige van hierdie modelle.

Die doel in hierdie proefskrif is om die vroeë aanvang van biofilm ontwikkeling te modeleer. Hierdie fase behels 'n bakteriële beweging na 'n oppervlak toe en die aanvanklike aanhegsel wat sal ontkiem in 'n biofilm. Ons gebruik 'n diffusievergelyking om 'n bakteriële kanslopie te beskryf, met geskikte randvoorwaardes. 'n Analities oplossing is verkry wat die bakteriële bevolkingsdigtheid beskryf as 'n funksie van tyd en posisie. Die model is ook onleed om te toets vir stabiliteit. Onafhanklik van die model, gee ons ook 'n reaksie-diffusievergelyking vir die beweging van waarnemings-molekules, wat insluit produksie deur die bakterieë en natuurlike afbreking.

Die laaste model wat ten toon gestel word is 'n Keller-Segel tipe model, wat die bakteriese en waarnemings-molekule dinamika koppel. In hierdie geval, neem die bakterieë 'n sydige kanslopie agter die waarnemings molekules aan. Die belangrikste deel van hierdie hoofstuk is die afleiding van die randvoorwaardes. Die klewerigheid van die bakterieë tot die oppervlak word vvorgestel deur nul-Dirichlet randvoorwaardes, terwyl die vergelyking wat waarnemingsmolekule gedrag by die koppelvlak beskryf bepaalde voorwaardes nodig het.

Bakterieë op die grensvlak produseer ook waarnemings-molekules wat diffundeer en afbreek. Om te verseker dat al hierdie eienskappe omvat is in 'n vergelyking is die aanname gemaak dat massa behoud bly. Ter afsluiting is numeriese simulasie van die model gedoen.

# Acknowledgements

I would like to express my sincere gratitude to the African Institute for Mathematical Sciences: first for the scholarship that funded my Masters and second, for what I learned throughout my post-graduate studies which has greatly impacted on my Masters results.

I extend my acknowledgement to my supervisors Dr. Aziz Ouhinou and Dr. Lafras Uys for their help and encouragement in making this work successful. I also thank Prof. Barry Green and Prof. Fritz Hahne for their advice and support throughout my Masters.

Finally, I acknowledge my family, including my beloved parents, for their patience and support during this whole period of study.

# Contents

# List of Figures

# List of Tables

# Nomenclature

Chapter 2 reviews three biofilm models from the literature. The notation in each section which deals with a particular model is the same as that of the original paper. Our work is presented in Chapter 3 and Chapter 4, where some notations from Chapter 2 might be reused in a different context. The list bellow will contain all the notations used throughout this thesis.

## In chapter 2

**For the one-dimensional continuum model**

| | | |
|---|---|---|
| $A$ | Sectional area | [ ] |
| $D_i$ | Diffusion coefficient of the i-th substrate | [ ] |
| $D_{l_i}$ | Diffusion coefficient in the bulk liquid | [ ] |
| $f_i$ | Volume fraction of the i-th species | [ ] |
| $g_i$ | Mass flux of the i-th species in the $z$-direction | [ ] |
| $L$ | Biofilm thickness | [ ] |
| $L_l$ | Substrate transfer layer thickness | [ ] |
| $ns$ | Substrates | [ ] |
| $nx$ | Microbial species | [ ] |
| $r_i$ | Substrate conversion rate | [ ] |
| $S_i$ | Substrate concentration | [ ] |
| $S_{l_i}$ | Substrate in the bulk liquid | [ ] |
| $u$ | Velocity of the microbial mass displacement | [ ] |
| $\mu o_i$ | Observed specific growth rate | [ ] |
| $\rho_i$ | Constant density for the i-th species | [ ] |
| $\sigma$ | Velocity | [ ] |

**For Continuum-discrete model**

| | | |
|---|---|---|
| $c(\vec{r}_i, t)$ | Nutrients concentration | [ ] |
| $c_r$ | Fixed rate of consuming nutrients | [ ] |
| $D_c$ | Nutrient diffusivity | [ ] |

| | | |
|---|---|---|
| $D_s$ | Communication chemicals diffusivity | [ ] |
| $s(\vec{r}_i, t)$ | Communication chemicals concentration | [ ] |
| $s_r$ | Fixed rate of communication chemicals production | [ ] |
| $\vec{r}_i$ | Walker's position | [ ] |
| $W_i$ | Walker's internal energy | [ ] |

# In chapter 3 and 4

### Spaces

| | |
|---|---|
| $\mathcal{L}^p$ | Lebesgue Space |

### Constants

| | |
|---|---|
| $\pi =$ | 3.141 592 654 |
| e = | 2.718 281 828 |

### Variables

| | | |
|---|---|---|
| $b(x,t)$, $B(x,t)$ | Bacterial density | $[\mathrm{kg/m^3}]$ |
| $b_{wall}(t)$, $B_{wall}(t)$ | Bacterial density | $[\mathrm{kg/m^3}]$ |
| $P(\mathbf{x},t)$ | Bacterial position | [ ] |
| $s(x,t)$, $S(x,t)$ | Sensing chemicals concentration | $[\mathrm{mol/m^3}]$ |
| $u(x,t)$ | Sensing chemicals concentration | $[\mathrm{mol/m^3}]$ |
| $\varepsilon(x,t)$ | Sensing chemicals concentration | $[\mathrm{mol/m^3}]$ |
| $\pi(x,t)$ | Intermediate function | [ ] |

### Parameters

| | | |
|---|---|---|
| $b_0$ | Bacterial initial density | $[\mathrm{kg/m^3}]$ |
| $c$ | Sensing chemicals production rate | $[1/\mathrm{s}]$ |
| $d$ | Step size | $[\mathrm{cm}]$ |
| $D_b$ | Bacterial diffusivity | $[\mathrm{m^2/s}]$ |
| $D_s$ | Sensing chemicals diffusivity | $[\mathrm{m^2/s}]$ |
| $K$ | Bacterial carrying capacity | $[\mathrm{kg/m^3}]$ |
| $L$ | Non-dimensional parameter | [ ] |
| $M$ | Non-dimensional parameter | [ ] |
| $N$ | Number of bacteria | [ ] |
| $a$ | Bacterial growth rate | $[1/\mathrm{s}]$ |
| $R$ | Circle radius | $[\mathrm{cm}]$ |
| $s_0$ | Sensing chemicals initial concentration | $[\mathrm{mol/m^3}]$ |

| | | |
|---|---|---|
| $T$ | Time steps | [ ] |
| $\alpha$ | Sensing chemicals production rate | [mol/kg s] |
| $\beta$ | Sensing chemicals production rate | [m mol/kg s] |
| $\varepsilon_0$ | Sensing chemicals initial concentration | [mol/m$^3$] |
| $\theta$ | Rotation angle | [rad] |
| $\lambda$ | Sensing chemicals degradation rate | [1/s] |
| $\mu$ | Rate at which bacteria get stuck | [1/m kg] |
| $\chi$ | Chemotactic coefficient | [m$^5$/mol s] |
| $\pi$ | Intermediate function | [kg/m$^3$] |

# Chapter 1

# The biology of bacterial biofilms

A biofilm is an aggregation of cells that accumulate on a surface. The cells live within a self-produced matrix generally composed of proteins, extracellular DNA and polysaccharides. Within a biofilm the cells are more cooperative with each other and behave differently than when they are in the free-state.

This thesis contains three main sections in addition to a discussion and conclusion at the end. In this chapter, we will give a biological description of bacterial biofilms. Our work will concern bacterial biofilms, that is prevalent in natural environments, industrial areas and hospital settings. In Chapter 2, we will study a variety of mathematical models of biofilm. We will discuss the results obtained, as well as the biological assumptions required to build the models. Chapter 3 introduces our own work, which is the mathematical modelling of the bacterial attachment to surfaces. The chapter consists of studying bacterial behaviour and sensing molecule motion separately. In Chapter 4, we consider a model of Keller-Segel type, to describe coupled bacterial chemotaxis and sensing molecule production. Keller-Segel type model describes bacterial directed movement towards an attractant or a repellent (chemotaxis).

Before looking at mathematical models of biofilms, it is necessary to understand the biology that outlines the modelling problem. We will describe biofilm components and explain the cellular behaviours within a biofilm. Some biofilms that are present in our daily life, will be cited and described. We will explain in detail the stages of biofilms formation. Then, end this chapter by giving our motivation to study biofilm.

## 1.1 What is a biofilm?

Bacterial biofilms are composed of clusters of bacteria. Biofilms can be made up of many different bacterial species. They surround themselves by a slime they secrete, generally composed of extracellular DNA, proteins, and polysaccharides in various configurations. Biofilms can also be made of other microorganisms, such as amoeba and algae.

Bacteria within a biofilm behave very differently compared to their counterparts in a free living state. Microbiologists have traditionally focused their experiments on planktonic bacteria that grow in laboratory cultures until it was realized, that most bacteria naturally aggregate as biofilms rather than living in the free state. And so, biofilms are interesting topics to be studied in microbiology [2]. It is estimated that the majority of bacteria live in biofilms. They provide an easy way for bacteria to find food and nutrients, as well as a high tolerance to antibiotics. In fact, bacteria of the same species are much more antimicrobial resistant, within a biofilm than in the free-swimming state. This is because of the high cooperation between the biofilm members. Two positive facts making bacteria choose to live within a biofilm instead of the planktonic state, are:

- The ability to differentiate into types that differ in their nutrient requirements. This means there are fewer competitors for a particular nutrient.
- When conditions deteriorate in a biofilm, some bacteria sacrifice themselves for the other bacteria to have a better life. They become planktonic cells once again, looking for another surface and build another biofilm in better conditions.

Biofilms exist wherever there is water attached to either an inert or living surface [3, 4]. They represent a prevalent mode of bacterial life in natural, industrial and hospital settings [5]. Some biofilms are beneficial, for example, sewage treatment plants, uses biofilms to remove contaminants from water. There are some biofilms that we may see every day, such as, the plaque on our teeth. The accumulation of bacterial micro-organisms on the surface of our teeth can cause dental diseases. The slippery slime on river stones that might result in water pollution. Biofilms can also be the cause of damage to contact lenses. Another place where biofilms thrive is in showers, since they provide a warm environment for bacteria to live in.

## 1.2 How do biofilms form?

Biofilms are omnipresent in natural and industrial settings. They are usually found on solid substrates submerged in, or exposed to, some aqueous solution [6, 7, 8]. Biofilms are small communities of bacterial cells that can grow on either, rich-nutrient or poor-nutrient surfaces. They can form floating mats on liquid surfaces and also on interfaces like air-water interfaces. The development a of biofilm is a multi-stage process, as shown in Figure 1.1.

There are five stages of the development of a biofilm, namely, the initial attachment, where the bacteria move toward either a living or non-living surface and attach to it. The irreversible attachment, the stage at which bacteria produce the polysaccharide matrix to facilitate their movement to a swarming

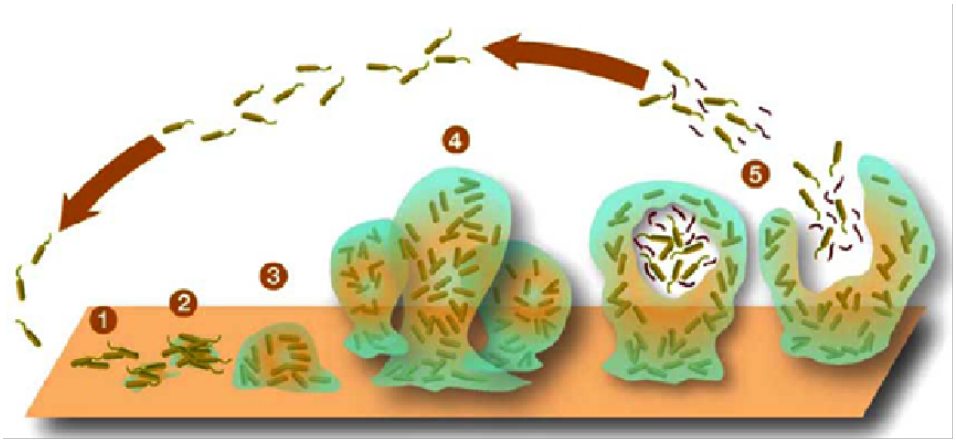


Figure 1.1: Description of the biofilm life cycle that occurs in five stages described in details in the text (see the last paragraph, page 2).
Source: http://prometheus.matse.illinois.edu/glossary/biofilms/.

rather than a free-state. The third stage is a period of maturation, which consists of growing as a initiated biofilm; bacteria proliferate and differentiate and also welcome other bacteria to join them. The fourth stage is a second maturation phase and the final stage in which bacteria disperse. This occurs when the environmental conditions worsen and bacteria choose to detach from the biofilm either to look for other surfaces or to join another biofilm.

## 1.3 Why study biofilm?

Biofilms are not all bad, they are a natural phenomenon that exists in our everyday environments and can be found even in extremely hot and cold environment. Biofilm can be beneficial, where it can be used

- to help in the clean up of an oil spill,
- in waste water treatment,
- in soil remediation.

Moreover, biofilms have a huge impact on our health. Many diseases and infections are caused by biofilms. These infections are usually much more difficult to treat than other non-biofilm infections resulting from the same microbes not in a biofilm state. Biofilms can also be found in common sites of infection in the human body. Once a biofilm reaches the bloodstream, it can easily cause infections in any surface of the human body. Bacterial biofilms may cause chronic infections which persist despite antibiotic therapy and are characterised by persistent inflammation and tissue damage [8, 9].

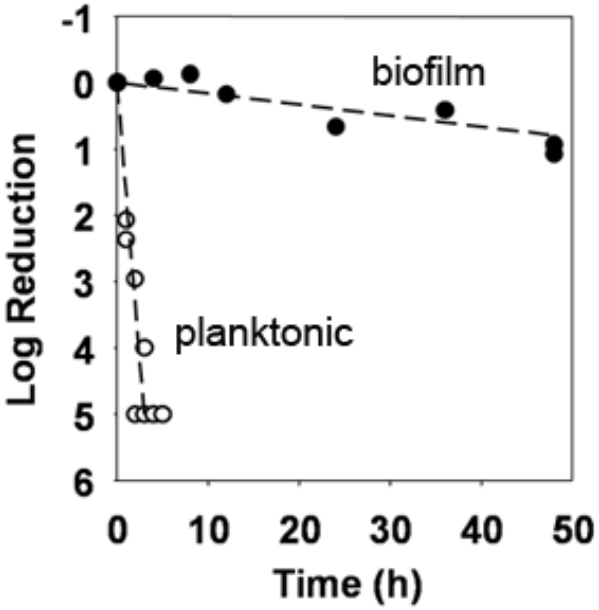


Figure 1.2: The reduction of bacteria in the presence of antibiotics in planktonic (empty circles) and biofilm (black circles) states. The antibiotic acting is *rifampin* and the bacteria is *Staphylococcus epidermidis*, for more explanations look at the second paragraph, page 4. Source [10]

Development of a biofilm is initiated by the reversible attachment of planktonic bacteria to a surface. At this stage the bacteria still show some susceptibility to antibiotics. In the next stage, which is the irreversible attachment, the biofilm grows in thickness to a mature biofilm. At this stage, biofilms show maximum tolerance to antibiotics.

*Staphylococcus epidermidis* is a normal part of the human skin flora. Figure 1.2 shows the tolerance of this bacteria to an antibiotic under different conditions. The y-axis shows the reduction of surviving number of bacteria on a logarithmic scale. Effectively, the antibiotics kills planktonic bacteria, while it has a little effect on biofilm even if after 2 days of continuous exposure.

Biofilm triggers inflammation and fibrosis (scar tissue formation) that make some breast implants become hard and distorted. Recently, in Tamboto *et al.* [11] small breast implants were implanted in a pig, where some of the implants are injected with small amount of bacteria. The injections are enough to cause a biofilm, but not enough to cause an infection. Thirteen weeks later, the animals were inspected for capsules to analyse any biofilm found on the breasts. 80.6% of the implants contained a biofilm that form a major capsular contractor (that is an abnormal response of the human body immune system to foreign materials). While some of the implants that were not injected with bacteria at the beginning also went on to form a capsule. This means they

also have biofilm formed, in this case the animal's own skin bacteria were the biofilm-forming organisms. This experimental study clearly links biofilms with capsular contractors in breast implantation.

It is the importance of biofilms and the complexity of its nature that make biofilm modelling a very challenging topic. In the following chapter we will present some biofilm models and discuss their advantages and disadvantages.

# Chapter 2

# A brief history of bacterial biofilm models

There are several approaches to modelling biofilms mathematically. We can model biofilm as a quantity that is continuous, discrete or both depending on the situation described. Some models simply describe the shape of biofilms; these have variously been described as looking like mushrooms, towers, fractals or some other pattern. Most of the models are computational, based on the movement and positions of bacteria within a well defined space.

Other models deal with biofilm growth. Either by considering the biofilm as a continuum mass growing, or, by taking into account the interaction between the individuals. These models vary from continuum to discrete models [1].

A third type, is those models that couple the biofilm and the surrounding environment, usually a fluid. These studies include biofilm sloughing and shear stress which also play an important role in biofilm life cycle. In general, these models are discrete-continuum or fully coupled biofilm-fluid models [8, 12, 13, 14].

The development of biofilm is a complicated process since it depends strongly on the surrounding environment. Over the last 30 years, good progress has been made in the mathematical modelling of bacterial biofilms. These models can be classified as shown in Table 2.1.

Table 2.1: Categories of biofilm models and time periods when they were actively developed.

| Models category | Time period | Reference |
|---|---|---|
| Low-dimensional continuum models | $1980 - 1985$ | [1] |
| Diffusion-limited aggregation models | $1981 - 1994$ | [8] |
| Continuum-discrete models | $1982 - 2006$ | [15] |
| Fully-coupled biofilm-fluid models | $1994 - 2008$ | [8, 16] |

An example of each of the first three categories will be presented and briefly reviewed in Sections, §2.1, §2.2 and §2.3.

## 2.1 One-dimensional continuum model

One-dimensional continuum models involve quantities assumed to be continuous, in time and on one-dimensional space. This category of models usually deals with steady-state biofilm growth dynamics, which includes: the biofilm's thickness; the spatial distribution of bacterial species, and substrate concentration; as example of these models we will present the work done by Wanner and Gujer [1].

Wanner and Gujer [1] (1985) presented a mathematical model involving a continuum description of biofilm. The multispecie biofilm model considers the biomass to be a continuum, by averaging the concentration of microbial species, as well as other similar quantities. It predicts the biofilm's thickness evolution, the spatial distribution of microbial species and substrate concentration, as well as, the biofilm detachment due to shear stress and sloughing [1]. This section will present the mathematical model, where all the parameters and variables used are given in Table 2.2 with their descriptions.

Table 2.2: State parameters and variables from a model presented by Wanner and Gujer [1].

| Parameter | Description |
|---|---|
| $A$ | Cross-sectional area |
| $D_i$ | Diffusion coefficient of the i-th substrate |
| $D_{l_i}$ | Diffusion coefficient in the bulk liquid |
| $f_i$ | Volume fraction of the i-th species (volume of the i-th specie over the total volume) |
| $g_i$ | Mass flux of the i-th species in the $z$-direction |
| $L$ | Biofilm thickness |
| $L_l$ | Substrate transfer layer thickness |
| $ns$ | Substrates |
| $nx$ | Microbial species |
| $r_i$ | Substrate conversion rate |
| $S_i$ | Substrate concentration |
| $S_{l_i}$ | Substrate in the bulk liquid |
| $u$ | Velocity of the microbial mass displacement |
| $\mu o_i$ | Observed specific growth rate |
| $\rho_i$ | Constant density for the i-th species |
| $\sigma$ | Velocity |

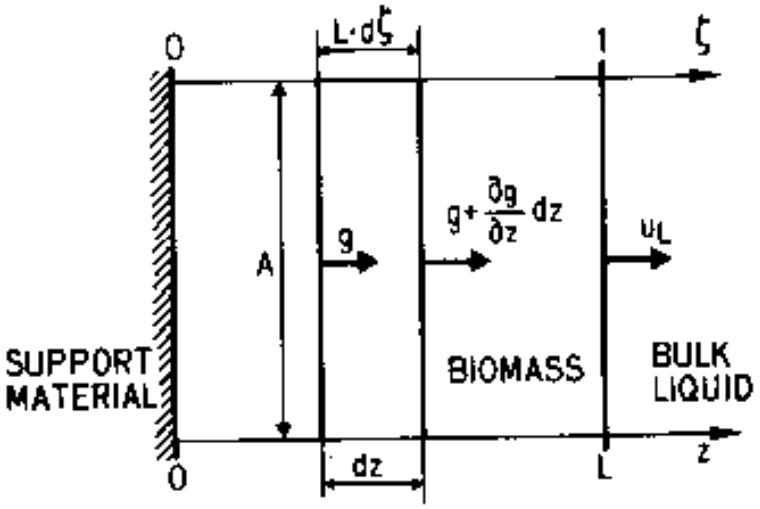


Figure 2.1: Flux of biomass through a differential volume element of an expanding biofilm. The scheme indicates the displacement of flux $g_i$, into and out of the differential volume $Adz$. Source [1]

Wanner and Gujer [1] assume that a biofilm is composed of $nx$ different microbial species within a well defined volume. The differential equation describing a mass balance of each species $i$ at a differential volume $Adz$ is given by,

$$\frac{\partial\left[Adz\rho_i f_i(t,z)\right]}{\partial t} = Adz\mu o_i(t,z)\rho_i f_i(t,z) + Ag_i(t,z) - A\left[g_i(t,z) + \frac{\partial g_i(t,z)}{\partial z}dz\right]. \tag{2.1.1}$$

This is equivalent to saying that, the change in the quantity $\rho_i f_i$ (mass balance of the species $i$) within the volume $Adz$ is equal to the species growth, with the appropriate amounts entering or leaving the volume added or removed (see Figure 2.1). Dividing (2.1.1) by $Adz\rho_i$ gives the differential equation,

$$\frac{\partial f_i}{\partial t} = \mu o_i f_i - \frac{1}{\rho_i}\frac{\partial g_i}{\partial z}. \tag{2.1.2}$$

The flux $g_i$ can be written as $g_i(t,z) = u(t,z)\rho_i f_i(t,z)$. Thus, Equation (2.1.2) becomes,

$$\frac{\partial f_i}{\partial t} = \left(\mu o_i - \frac{\partial u}{\partial z}\right) f_i - u\frac{\partial f_i}{\partial z}. \tag{2.1.3}$$

By summing over all the $nx$ microbial species, Equation (2.1.3) will be,

$$\frac{\partial u(t,z)}{\partial z} = \bar{\mu}o(t,z), \quad \text{where } \bar{\mu}o(t,z) = \sum_{i=1}^{nx}\mu o_i(t,z)f_i(t,z). \tag{2.1.4}$$

Then we determine the velocity $u$ by the mean observed specific growth rate of the biomass $\bar{\mu}o(t,z)$ as,

$$u(t,z) = \int_0^z \bar{\mu}o(t,z')dz', \tag{2.1.5}$$

where $u(t,0) = 0$. The biofilm thickness $L$, changes as the biofilm grows or shrinks while the film-water interface moves at a velocity defined by,

$$u_L(t) \equiv \frac{dL(t)}{dt}, \tag{2.1.6}$$

with respect to the film-support interface. The velocity of the film-water interface is expressed by defining $\sigma(t)$ as the velocity at which biomass is exchanged between biofilm and bulk liquid, so that Equation (2.1.5) becomes,

$$u_L(t) = \int_0^L \bar{\mu}o(t,z')dz' + \sigma(t). \tag{2.1.7}$$

Equations (2.1.3) and (2.1.4) give the mass balance equation for $f_i$,

$$\frac{\partial f_i}{\partial t} = \left[\mu o_i(t,z) - \bar{\mu}o_i(t,z)\right] f_i(t,z) - u(t,z)\frac{\partial f_i(t,z)}{\partial z}, i = 1, ..., nx-1. \tag{2.1.8}$$

On the other hand, the bulk liquid is assumed to contain $ns$ different substrates, so that a mass balance for the substrate $i$ can be written as:

$$\frac{\partial S_i(t,z)}{\partial t} = r_i(t,z) + \frac{\partial}{\partial z}\left(D_i\frac{\partial S_i(t,z)}{\partial z}\right), \quad i = 1, ..., ns, \tag{2.1.9}$$

with $S_i$ as the concentration, $r_i$, the observed conversion rate and $D_i$, the diffusion coefficient of each substrate $i$. Equation (2.1.9) shows the diffusion and production of the substrate $i$. The boundary conditions used are, for the film-support interface ($z = 0$),

$$\frac{df_i}{dt} = (\mu o_i - \bar{\mu}o)f_i, \qquad \frac{\partial S_i}{\partial z} = 0,$$

due to the no-flux at this interface. For the film-water interface ($z = L$),

$$\frac{\partial S_i}{\partial z} = \frac{LD_{l_i}}{L_l D_i}(S_{l_i} - S_i) \text{ or } S_i = S_{l_i},$$

The steady-state analysis of the presented mathematical model predicts that the spatial distribution of a microbial species can be described by one or more layers, whether the biofilm is homogeneous (mono-species biofilm) or mixed (multi-specie biofilm). This result is valid for any given situation, which means whether the species compete only for space or only for substrate. The situation chosen for numerical simulations is a heterotrophic-autotrophic

competition for the common resources, space and oxygen. Heterotrophic and autotrophic are both microbial metabolisms that consist of getting carbon, from, respectively, organic compounds and carbon dioxide. The study considered five cases, namely, 1) unrestricted growth; 2) changes in bulk liquid substrate concentration; 3) biomass shear; 4) biomass sloughing; and 5) biofilm in a completely mixed reactor with external mass transfer resistance. In each case, the the biofilm's thickness evolution with time and the substrates removal from the bulk liquid were presented [8, 1]. The results show that the biofilm composition depends on the microbial species kinetics, the concentration of substrate, and the reactor configurations and a biomass detachment mechanism.

The advantages of the model are that it involves multiple microbial species and substrates. It looks at the biofilm composition and growth, which makes it one of the very interesting biofilm models.

The model has some disadvantages, like the fact that it did not consider individual behaviours which play an important role in biofilm formation, especially in the very early biofilm stages.

In the next section we will give an example of biofilm computational models.

## 2.2 Diffusion limited aggregation model

Biofilm shape can be modelled using Diffusion limited aggregation model (DLA). This is a computational model consisting of particles performing a random walk to form aggregations. DLA models are used to describe the shape of fractal-like biofilms [8].

The rule of a DLA algorithm consists of considering a square lattice on a plane, where a particle is set to be the origin. A second particle is released far from the origin , that moves randomly (see Figure 2.2 left graph). When it reaches the origin's neighbouring sites, it becomes stationary. A third particle is released and it moves until it arrives at the neighbouring site near by the cluster made of the two previous particles. The process is repeated continuously until the cluster grows as a randomly-branched structure. The right graph on Figure 2.2 is a result of computational simulation of a DLA algorithm.

*Bacillus subtilis*(*B.subtilis*) bacteria are able to grow at a very low nutrient level on an agar plate to form randomly-branched structures that could be compared to numerical results of a DLA model (see Figure 2.3).

Despite the good agreement between the DLA models and experimental results, we should mention that this type of model does not include any of the environmental conditions that play an important role in biofilm formation in real life. This type of model studies the shapes of biofilm based on simple assumptions.

However, there exist other type of models that are more realistic and in-

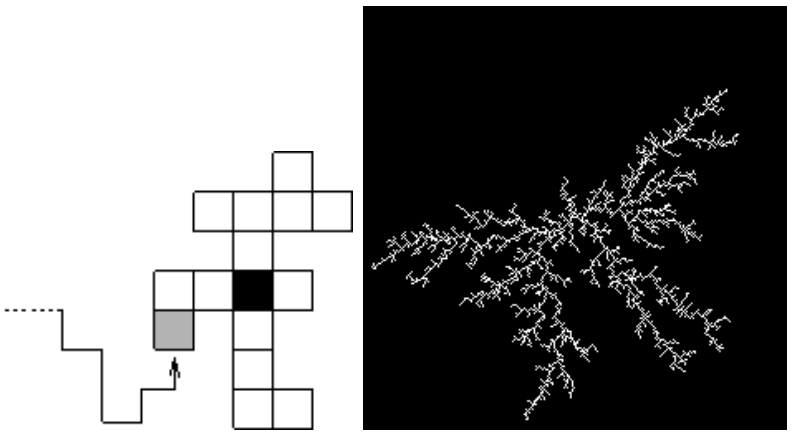

Figure 2.2: A DLA computational model. The left figure shows the rule of a DLA growth, where the solid cell is the origin, the grey cell is a new cell released (see paragraph 2, page 10). The right figure shows the computer simulation of a DLA model, where the cluster is consisting of 100, 000 particles.

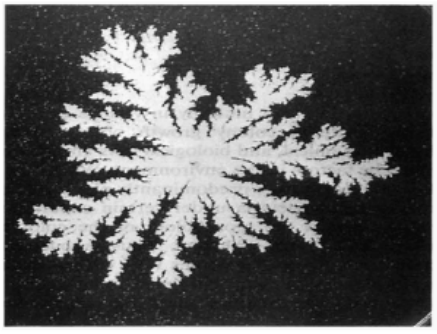

Figure 2.3: A fractal-like biofilm made by *B. subtilis* bacteria growing on an agar plate under very low nutrient conditions. The colony was photographed 21 days after inoculation. Its diameter is about 47 mm. Source: [8]

clude more biological features of biofilms. Among these we present a continuum-discrete model in the following section.

## 2.3 Continuum-discrete model

Discrete-continuum models (also called Cellular Automaton models) consist of a regular grid of cells, each in one of a finite number of states. The grid is in any finite number of dimensions. The state of a cell at time $t$ depends on the states of its neighbourhood cells at time $t-1$, where time is also discrete. Each time the rules are applied to the whole grid and a new generation of

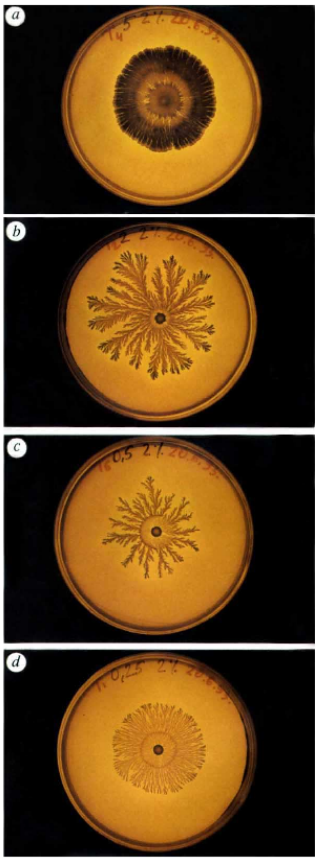


Figure 2.4: Observed patterns of *B. subtilis* grown colonies (See text in the last paragraph, page 12 for details), Source [17].

cells is created. In this section we will review this type of model by reviewing Ben Jacob *et al.* [17].

The continuum-discrete model includes bacterial movement and the diffusion of nutrients. The bacteria are presented by small aggregations (called walkers) rather than individuals. The study will be based on a comparison between experimental results and numerical simulations for the mathematical model. We will start by a description of the experiment done on *B. subtilis* bacteria.

Figure 2.4 shows bacterial colonies grown under different conditions. The nutrients level ranges from a very low level (d) to a very rich mixture (a). The medium vary from a soft agar (a) to a hard agar (d). The growth started with a droplet inoculation at the center of the Petri dishes. The growth pattern described are of bacteria derived from *B. subtilis* [15, 17]. The colonies shapes vary as growth conditions are varied (see Figure 2.4). At a high peptone level, the pattern is very dense with wide branches. The patterns become more ramified (b and c), as the peptone level is decreased; even at lower peptone

levels, the patterns become denser again (d), this phenomenon is expected to result from chemotaxis signalling.

Ben Jacob *et al.* [17] included the following generic features in the model: the diffusion of nutrients and substrates (as continuous quantities), the movement of bacteria described by walkers positions (discrete quantity). The walkers perform a random walk within a well-defined envelope. The local intracellular communication between bacteria was also included to perform the last feature found in the experiment.

The biological assumptions involved in this model are summarized as follows:

- Movement of the nutrient is obtained by solving the diffusion equation for nutrient concentration $c$, on a triangular lattice.
- Bacteria are presented by walkers that are small aggregations of bacteria, each of which is viewed as a mesoscopic unit.
- Each walker is presented by its location $\vec{r_i}$, and an interval of degree of freedom (' internal energy $W_i$ ').
- The internal energy of walkers is increased by consuming nutrients at a fixed rate $c_r$, when food is abundant. Otherwise, the walker consumes the available amount of food. The walker loses its internal energy at a fixed rate $e$.
- When there is lack of food for an interval of time (so that $W_i$ drops to zero), the walker becomes stationary. When food is again available, $W_i$ increases, and when it reach a threshold $t_r$, the walker proliferates (reproduction).

The nutrient concentration is given by the solution to,

$$\frac{\partial c(\vec{r},t)}{\partial t} = D_c \nabla^2 c(\vec{r},t) - \sum_{\text{active walkers}} \delta(\vec{r}-\vec{r_i}) \min(c_r, c(\vec{r},t)), \tag{2.3.1}$$

where $D_c$ is the diffusion constant of the nutrients, the equation shows the diffusion and consumption of the nutrient by the active walkers. The evolution of $W_i$ in time is represented by,

$$\frac{dW_i}{dt} = \min(c_r, c(\vec{r_i},t)) - e. \tag{2.3.2}$$

The active walkers move randomly within a well-defined envelope at step-size $d$ and angle $\theta \in [0, 2\pi]$. Thus, we obtain the new location $\vec{r'_i}$ by,

$$\vec{r'}_i = \vec{r_i} + d(\cos\theta, \sin\theta). \tag{2.3.3}$$

The numerical results show the pattern shapes that differ as the peptone level and the agar concentration changed. At high peptone levels the patterns are compact and change to fractal when nutrient level decreases, which is similar to the obtained experimental results. While, if the peptone level is fixed and the agar concentration varies, the obtained numerical patterns become more ramified as the agar concentration is increased.

Comparing the numerical results of the model and the experimental results some differences are found. The most important one is the bacterial ability to develop organized patterns at very low peptone levels. Compare this to the graph (d), Figure 2.4, which is missing by this model. The reason why the model did not capture the last feature, is because as the environmental conditions become worse (low nutrients or hard surface), the colony become highly cooperative. This fact makes the intracellular communication between the individuals needed to be included into the model.

For that a simple version of chemotactic communication is included in the model, in the hope of identifying the generic feature that it induces. In order to fix that another assumption is taken into account. At low peptone levels, the walkers become stationary and start producing a signalling molecules at a fixed rate $s_r$ to drive active walkers away from the low nutrient region. The active walkers consume the chemical at a fixed rate $c_c$. The communication chemicals concentration is represented by,

$$\begin{aligned}\frac{\partial s(\vec{r},t)}{\partial t} &= D_s\nabla^2 s(\vec{r},t) + \sum_{\text{stationary walkers}} \delta(\vec{r}-\vec{r_i})s_r \\ &- \sum_{\text{active walkers}} \delta(\vec{r}-\vec{r_i})\min(c_c, s(\vec{r},t)),\end{aligned}$$

where the equation shows the diffusion, consumption and production of communication chemicals by the walkers. Bacterial movement changes from a pure random walk to a biased random walk, in the direction of the signalling molecules. After including the bacterial communication into the model the results changed so that the patterns formed at low peptone level are denser than obtained in experiment. This simplified version is sufficient to capture the feature needed but a more realistic model would include a dependence on the rates $s_r$ and $c_c$, on the concentration of nutrients.

In this chapter, we have looked at the variety of mathematical models of biofilms. Each particular example has its own assumptions and its own computational and mathematical tools used. These models usually considers that biofilm's structure is determined by the substrate concentration and bacterial movement. This fact make theme generally governed by the diffusion process. However, the hydrodynamics of the bulk fluid plays an important role in shaping the structure of biofilms. Here comes the importance of biofilm-fluid models, which are governed by physical concepts such as, momentum conservation and transfer, mass conservation, fluid velocity and viscosity [8, 18].

In Chapter 3, we will model biofilm in a different way, by looking at the early stages of its formation. We will consider bacterial movement toward surfaces that is the first step of biofilm formation, and give the biological description of bacterial behaviour during this step. The tools used in our work will be similar to those used in the models discussed in this chapter. A good understanding of these models will inform our work even if the models are dealing with different stages of biofilm. We are interested in the early stage of biofilm, but the mathematical tools used remain similar.

# Chapter 3

# Modelling bacterial motility, surface attachment and sensing molecule distribution

In this chapter we will present a new contribution to the field of biofilm modelling. This phenomenon involves two main elements, bacteria and sensing molecules. Two models are presented separately, describing bacterial motility and molecular diffusion. The models are studied by: analysing the steady-state and stability properties, and; performing a numerical simulation. The coupled model that considers the interactions between bacteria and sensing molecules will be described in Chapter 4.

First, we will give a more detailed biological description of the biofilm stage we are modelling.

## 3.1 Attachment of bacteria to surfaces

In the natural world, bacteria are more likely to grow and survive in organized communities than to be found as isolated cells [19]. In the life and times of the biofilm, the initial adhesion of the planktonic bacterial cell to a conditioned surface is considered as a random event [20]. This free-living bacteria produce sensing molecules as they move through the bulk fluid. These chemicals become significantly concentrated as the population of bacteria grows, they diffuse radially away from the floating cells and get reflected once they reach the surfaces. At this stage, bacteria sense their proximity to these surfaces because diffusion had become limited on that side [5, 16, 21]. The bacteria keep moving toward the nearest surface where they get stuck, resulting in more sensing molecules produced at the boundaries. This increased production causes an escalation in the recruitment of bacteria to the pioneering colonies, which will merge to form the biofilm. Figure 3.1 illustrates this behaviour that will be the subject of our mathematical modelling.

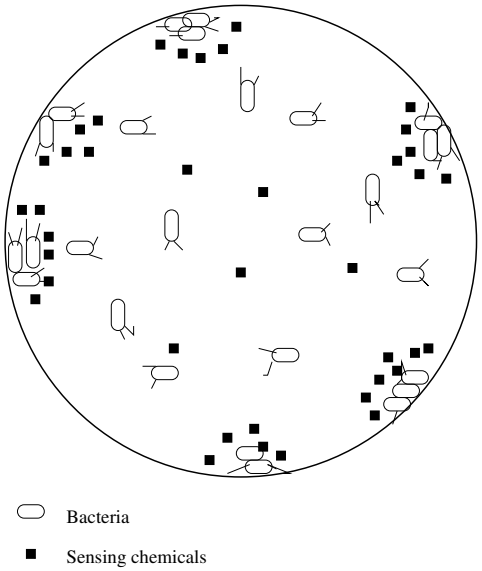


Figure 3.1: Illustration of bacterial attachment to the surface. Bacteria (represented by the oval empty circles) are distributed within a circle where the surface is situated in the circle boundaries. They move randomly and produce sensing molecules (black squares), to sense their proximity to the surface. Once bacteria reach the surface it get stuck and keep producing the sensing molecules to attract other bacteria

## 3.2 Assumptions that shape the model

Before we start presenting our models, we give a brief description of how we link the biology of biofilm formation with the mathematics of modelling. In the first two models, the phenomenon that we want to model includes bacterial random walk toward the surface. This will be presented by the diffusion equation that has as a variable, bacterial density which depends on time and space, and as a parameter, bacterial diffusivity coefficient.

In addition to that, bacteria get stuck once the surface is reached. To present this phenomenon mathematically we will consider that bacteria disappear from the free-space once they reach the surface. This will be represented by zero-Dirichlet boundary conditions. The bacteria that reached the surface will belong to another bacterial population situated on the boundaries and depends only on time.

For the model representing sensing molecules, we describe sensing molecules random movement by a diffusion equation for their concentration that depends on time and space. The sensing molecules degrades, so our mathematical model will contain a function to describe that. This function will depend on sensing molecules concentration and the fixed rate of degradation. The sensing chemicals are assumed to have a source at the boundaries, mathematically this

will be presented by constant-Dirichlet boundary conditions.

Furthermore, the model assumptions will change to considering both bacteria and sensing molecules in the same mathematical model, and involving sensing molecules production by both free-bacteria and stuck-bacteria. The movement of free-bacteria will change from a pure random walk to a biased random walk toward sensing molecules. This will introduce a new concept called chemotaxis to our model, which become of Keller-Segel type described later in Chapter 4. The production of sensing molecules will occur in the free-space and at the surface, in both places it will be represented by functions that depend on bacterial densities and fixed rates of production. For sensing molecules degradation and bacterial stickiness, they will be defined similarly. While the function describing sensing chemicals at the surface (boundary conditions) will be explained in details in Chapter 4, Section §4.2 and it will be our main contribution in this work. Up to now we did not consider bacterial growth, this will be the subject in the next chapter.

## 3.3 Modelling bacterial motility and attachment with a diffusion equation

The bacteria is performing a random walk, also named, Brownian motion, within a well-bounded medium, and once they reach the boundaries they get stuck. One way of modelling this behaviour is to make use of the Fokker-Planck equation for the description of Brownian motion of a particle, (in our case the bacterium), in a fluid [3, 22, 23].

In one spatial dimension $x$, the Fokker-Planck equation for a process with diffusion $D(x,t)$ and without drift is,

$$\frac{\partial}{\partial t}b(x,t) = \frac{\partial^2}{\partial x^2}[D(x,t)b(x,t)]. \tag{3.3.1}$$

Equation (3.3.1) is also called Diffusion equation which; by considering a linear bacterial diffusivity, $D_b$, could be written as,

$$\frac{\partial}{\partial t}b(x,t) = D_b\frac{\partial^2}{\partial x^2}b(x,t). \tag{3.3.2}$$

The biological assumptions considered by the mathematical model are summarized as follows:

- Bacteria perform a random walk within a normalized one-dimensional space $[0,1]$.
- Surface is located at the boundaries.
- Bacteria stick to the surface once reached [21].

We consider that free-bacteria get absorbed by the surface (wall) at the boundaries, so that zero-Dirichlet boundary conditions are used to express that absorbed bacteria are actually the bacteria stuck to the walls. As a result, these bacteria disappear from the free-space and appear at the surface as wall-bacteria, named later on $b_{wall}$.

$$\frac{\partial b}{\partial t} = D_b \frac{\partial^2 b}{\partial x^2}, \qquad 0 < x < 1, t > 0, \tag{3.3.3}$$

$$b(0,t) = b(1,t) = 0, \qquad t > 0, \tag{3.3.4}$$

$$b(x,0) = b_0, \qquad 0 < x < 1, \tag{3.3.5}$$

where $D_b$ is bacterial diffusivity and $b_0$ is a positive constant describing bacterial initial density, the problem is well defined and has a positive solution [24] for positive initial condition.

We use the separation of variables method [25] to solve analytically Equation (3.3.3). We start with,

$$b(x,t) = X(x)T(t), \tag{3.3.6}$$

and we note $-\lambda$ the separation constant to get the two following qualities,

$$\frac{X''}{X} = \frac{T'}{D_b T} = -\lambda, \tag{3.3.7}$$

which lead to the two ordinary differential equations,

$$X'' + \lambda X = 0, \tag{3.3.8}$$

$$T' + D_b \lambda T = 0. \tag{3.3.9}$$

Before solving Equations (3.3.8) and (3.3.9), we note that the boundary conditions (3.3.4) applied to Equation (3.3.6), are,

$$b(0,t) = X(0)T(t) = 0, \quad b(1,t) = X(1)T(t) = 0. \tag{3.3.10}$$

Expecting that $T(t) \neq 0$ for $t > 0$, implies that the boundary conditions are only satisfied if,

$$X(0) = 0 \quad and \quad X(1) = 0.$$

For the solution of (3.3.8), we shall consider three cases, namely,

**case 1:** $\lambda < 0$ We write $\lambda = -\alpha^2$ where $\alpha$ denotes a positive number, the auxiliary equation of Equation (3.3.8) is given by,

$$m^2 - \alpha^2 = 0,$$

its roots are, respectively, $m_1 = \alpha$ and $m_2 = -\alpha$. Since we are working in a finite domain, the solution is hyperbolic and given by,

$$X(x) = A\cosh(\alpha x) + B\sinh(\alpha x),$$

where $A$ and $B$ are constants in $\mathbb{R}$ which become $A = 0$ and $B = 0$ when we apply the boundary conditions. As a result, the solution of Equation (3.3.8) is the trivial one,

$$X \equiv 0,$$

which means,

$$b(x,t) \equiv 0,$$

as well. □

**case 2:** $\lambda = 0$ The solution is linear written as,

$$X(x) = Ax + B, \tag{3.3.11}$$

which together with the boundary conditions, leads to $A = 0$ and $B = 0$. Then the solution is again the trivial one. □

**case 3:** $\lambda > 0$ In this case, we write $\lambda = \alpha^2$, where $\alpha$ is a positive number. The auxiliary equation is of the form,

$$m^2 + \alpha^2 = 0, \tag{3.3.12}$$

which has complex roots $m_1 = i\alpha$ and $m_2 = -i\alpha$. The general solution of (3.3.8) is elliptic of the form,

$$X(x) = A\cos(\alpha x) + B\sin(\alpha x), \tag{3.3.13}$$

as before, by using the boundary condition $X(0) = 0$, we get that $A = 0$, so,

$$X(x) = B\sin(\alpha x). \tag{3.3.14}$$

Using $X(1) = 0$ we get that $B\sin(\alpha) = 0$, which gives us two cases, either $B = 0$ and in this case,

$$X \equiv 0, \tag{3.3.15}$$

or if we require $B \neq 0$, then $\sin\alpha = 0$ is satisfied whenever $\alpha$ is an integer multiple of $\pi$,

$$\alpha = n\pi \quad \Leftrightarrow \quad \lambda_n = \alpha_n^2 = n^2\pi^2, \quad n = 1, 2, 3, ... \tag{3.3.16}$$

Then for any $B \neq 0$, the solution of (3.3.8) is given by,

$$X(x) = B\sin(n\pi x), \tag{3.3.17}$$

and because of the linearity of Equation (3.3.8), the sum of the solutions over $n$ is also a solution.

Hence, (3.3.8) has non-trivial solutions when,

$$\alpha = n\pi, \quad \Leftrightarrow \quad \lambda_n = \alpha_n^2 = n^2\pi^2, \quad n = 1, 2, 3, .... \tag{3.3.18}$$

These values of $\lambda$ are called eigenvalues of the problem, and the solutions $X(x) = B\sin(n\pi x)$ are called the associated eigenfunctions. On the other hand, solving (3.3.9) gives rise to,

$$T(t) = C\exp(-n^2\pi^2 D_b t). \tag{3.3.19}$$

Finally, we obtain,

$$b_n = X(x)T(t) = A_n\exp(-n^2\pi^2 D_b t)\sin(n\pi x). \tag{3.3.20}$$

Therefore, by superposition principle, the solution of Equation (3.3.3) is given by,

$$b(x,t) = \sum_{n=1}^{\infty} b_n = \sum_{n=1}^{\infty} A_n\exp(-n^2\pi^2 D_b t)\sin(n\pi x). \tag{3.3.21}$$

The final step is to apply the initial conditions, namely,

$$b(x,0) = \sum_{n=1}^{\infty} b_n = \sum_{n=1}^{\infty} A_n\sin(n\pi x) = b_0, \tag{3.3.22}$$

We convert to Fourier series by multiplying the equation by $\sin(m\pi x)$ where $m$ is an integer, and integrating between 0 and 1. Thus, we obtain,

$$A_n = 2\int_0^1 b_0\sin(n\pi x)dx = \frac{2b_0}{n\pi}(1-\cos(n\pi)),$$

for all positive integers, $n$.

Finally, the solution is,

$$b(x,t) = \sum_{n=1}^{\infty}\frac{2b_0}{n\pi}(1-\cos(n\pi))\exp(-n^2\pi^2 D_b t)\sin(n\pi x), \tag{3.3.23}$$

it describes the movement of bacteria in the free-space. While the bacteria stuck to walls, $b_{wall}(t)$ at a given time $t$, will be calculated by the following equation,

$$b_{wall}(t) = \int_0^1 b_0 dx - \int_0^1 b(x,t)dx = b_0 - \int_0^1 b(x,t)dx, \tag{3.3.24}$$

because $b_0$ is a constant and $\displaystyle\int_0^1 dx = 1$, this result is supported by the conservation of mass law. □

Now we found the explicit solutions our mathematical model describing bacterial density. In the next section we will study the convergence and stability of the steady state solution.

## 3.4 Convergence and stability analysis of the bacterial diffusion equation

**Proposition 3.4.1.** *Under the presented assumptions we show that the bacterial population is almost zero everywhere in the free-space* $(0,1)$*. For that, we show the following limit,*

$$\lim_{t\to\infty} b_{wall}(t) = b_0 \Leftrightarrow \lim_{t\to\infty} \int_0^1 b(x,t)dx = 0.$$

*Proof.* We set,

$$b_n(x,t) = \frac{2b_0}{n\pi}(1-\cos(n\pi))\exp(-n^2\pi^2 D_b t)\sin(n\pi x),$$

so that,

$$b(x,t) = \sum_{n=1}^{\infty} b_n(x,t) = \sum_{n=1}^{\infty} \frac{2b_0}{n\pi}(1-\cos(n\pi))\exp(-n^2\pi^2 D_b t)\sin(n\pi x).$$

We need to compute,

$$\lim_{t\to\infty} \int_0^1 b(x,t)dx = \lim_{t\to\infty} \int_0^1 \left(\sum_{n=1}^{\infty} b_n(x,t)\right) dx.$$

Let $t_0 > 0$, so for $n \in \mathbb{N}^*$, and $t \geq t_0$ we have that,

$$\begin{aligned} b_n(x,t) &\leq \frac{4b_0}{\pi}\exp(-n^2\pi^2 D_b t), \\ &\leq \frac{4b_0}{\pi}\exp(-\pi^2 D_b t)\exp(-(n^2-1)\pi^2 D_b t), \\ &\leq \frac{4b_0}{\pi}\exp(-\pi^2 D_b t)\exp(-(n^2-1)\pi^2 D_b t_0). \end{aligned}$$

Thus for $t \geq t_0$,

$$\begin{aligned} \sum_{n=1}^{\infty} b_n(x,t) &\leq \frac{4b_0}{\pi}\exp(-\pi^2 D_b t)\sum_{n=1}^{\infty}\exp(-(n^2-1)\pi^2 D_b t_0), \\ \int_0^1 \sum_{n=1}^{\infty} b_n(x,t)dx &\leq \frac{4b_0}{\pi}\exp(-\pi^2 D_b t)\sum_{n=1}^{\infty}\exp(-(n^2-1)\pi^2 D_b t_0). \end{aligned}$$

Since,

$$\lim_{t\to\infty}\exp(-\pi^2 D_b t) = 0,$$

we conclude that,

$$\lim_{t\to\infty} \int_0^1 b(x,t)dx = \lim_{t\to\infty} \int_0^1 \sum_{n=1}^{\infty} b_n(x,t)dx = 0,$$

**Definition** Let $f$ be a well defined function. We define the norm of $f$ on the Lebesgue space $\mathcal{L}^p(0,1)$ by:

$$\| f \|_p := \left( \int_0^1 | f |^p \, d\mu \right)^{1/p} < \infty,$$

where $1 \leq p < \infty$ and $\mu$ is the space measure.

**Corollary 3.4.2.** *The solution $b(x,t)$ converges to the trivial stable steady-state in $\mathcal{L}^1(0,1)$,*

$$\lim_{t\to\infty} \int_0^1 b(x,t)dx = 0 \Leftrightarrow \lim_{t\to\infty} \| b(x,t) - 0 \|_{\mathcal{L}^1(0,1)} = 0. \tag{3.4.1}$$

□

In the following we will plot bacterial density and emphasize the analytical results.

## 3.5 Numerical illustration of bacterial densities

To illustrate the analytical solution, we plot the density evolution in time (see Figure 3.2); the bacterial density in the free-space ($\int_0^1 b(x,t)dx$) and at the walls ($b_{wall}(t)$) can be seen.

With the given parameter values, the bacterial density is decreasing in the free-space and increasing at the surface and the total density sums to $b_0$ at each time.

At around $T \approx 10^3$, half of the population reach the boundaries, where at $T \approx 10^4$, most of the population are stuck to the boundaries and negligible number of bacteria are free which agree with analytical result,

$$\lim_{t\to\infty} \int_0^1 b(x,t)dx = 0.$$

In the next section, the same analysis will be done to study the dynamics of sensing molecules.

## 3.6 Sensing molecule distribution modelled as a reaction-diffusion process

Before considering the coupled model that involve both bacteria and sensing molecules, we may model the sensing molecules on their own to look at the evolution of their distribution profile then, the bacterial distribution will be driven by the concentration profile of sensing molecules. The mathematical model will be derived under the following biological assumptions:

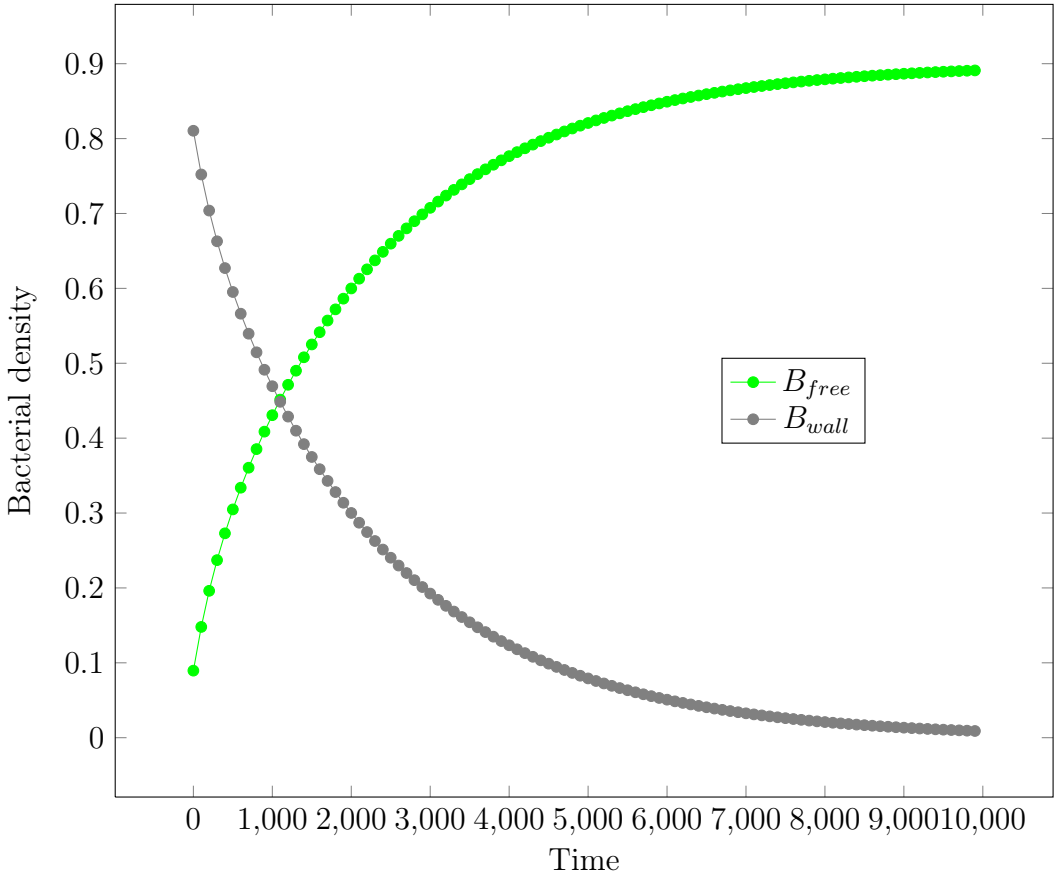


Figure 3.2: Bacterial density evolution over time for both bacteria in the free-space and bacteria on the surface. The total bacteria were in the free-space in the starting point $t = 0$. As time gets larger, the free-bacterial density decreases to make the stuck-bacterial density increase since more bacteria attach to the surface. The parameters used are $D_b = 0.025$ and $b_0 = 0.5$.

- sensing molecules diffuse within a one-dimensional space $[0, 1]$.
- sensing molecules degrade.
- A fixed source exists at the surface (walls) situated at the boundaries.

We consider the following boundary value problem,

$$\frac{\partial s}{\partial t} = D_s \frac{\partial^2 s}{\partial x^2} - \lambda s, \qquad 0 < x < 1,\ t > 0, \tag{3.6.1}$$

$$s(0,t) = s(1,t) = c, \qquad t > 0, \tag{3.6.2}$$

$$s(x,0) = s_0, \qquad 0 < x < 1, \tag{3.6.3}$$

where $D_s$ is the sensing molecules diffusivity, $\lambda$ is a degradation coefficient, $s_0$ is the initial sensing molecules concentration and $c$ is the production rate at the walls.

The boundary conditions used are called inhomogeneous Dirichlet boundary conditions. Using a simple change of variables we can write Equation (3.6.1) as an inhomogeneous equation in order to get homogeneous Dirichlet boundary condition that are easier to deal with. For that we set,

$$u(x,t) = s(x,t) - c \tag{3.6.4}$$

thus Equations (3.6.1), (3.6.2) and (3.6.3) are equivalent to,

$$\frac{\partial u}{\partial t} = D_s \frac{\partial^2 u}{\partial x^2} - \lambda u - \lambda c, \qquad 0 < x < 1,\ t > 0, \tag{3.6.5}$$

$$u(0,t) = u(1,t) = 0, \qquad t > 0, \tag{3.6.6}$$

$$u(x,0) = s_0 - c = u_0, \qquad 0 < x < 1. \tag{3.6.7}$$

Since the amount of sensing chemicals become interesting when more bacteria are attached. We need to look at the long time behaviour of sensing molecules rather than finding the exact solution. This results to a steady-state analysis performed in the next section.

## 3.7 Distribution of sensing molecules at equilibrium

In this part, we will illustrate sensing molecules dynamics as time gets larger. In order to do so, we need to find the stationary and study its stability. We set,

$$\frac{\partial u}{\partial t} = 0 \Leftrightarrow D_s \frac{d^2 u(x)}{dx^2} - \lambda u(x) - \lambda c = 0. \tag{3.7.1}$$

The aim of this part is to transform a second-order ordinary differential equation into a system of two first-order ordinary differential equations, for that we consider the following change of variables,

$$\frac{du}{dx} = v, \tag{3.7.2}$$

$$\frac{dv}{dx} = \frac{d^2 u}{dx^2} = \frac{\lambda}{D_s} u + \frac{\lambda}{D_s} c, \tag{3.7.3}$$

we define,

$$X = \begin{pmatrix} u \\ v \end{pmatrix} \Rightarrow X' = \begin{pmatrix} u' \\ v' \end{pmatrix}$$

so that we can write Equations 3.7.2 and 3.7.3 as follows,

$$X' = AX + f, \tag{3.7.4}$$

$$X(x_0) = X_0, \tag{3.7.5}$$

where,

$$A = \begin{pmatrix} 0 & 1 \\ \frac{\lambda}{D_s} & 0 \end{pmatrix} \quad f = \begin{pmatrix} 0 \\ \frac{\lambda}{D_s} \end{pmatrix}.$$

**Definition** A matrix function $\Phi(x)$ is a fundamental matrix of the system $X' = A(x)X$ if it solves the matrix system $X' = A(x)X$ and $\det \Phi(x) \neq 0$.

**Theorem 3.7.1.** *[26] If $f$ is continuous and $\Phi$ is a fundamental matrix of $X' = AX + f$, then,*

$$X' = AX + f \tag{3.7.6}$$

*has a particular solution,*

$$X_p(x) = \int_0^x \Phi(x-s)f(s)ds, \tag{3.7.7}$$

**Theorem 3.7.2.** *[26] The initial-value problem,*

$$X' = AX + f \quad X(x_0) = X_0 \tag{3.7.8}$$

*has the unique solution,*

$$X(x) = X_p(x) + \Phi(x)X_0, \tag{3.7.9}$$

*where $\Phi$ is a normalized fundamental matrix of the complementary system, $X' = AX$ at $x_0$ and,*

$$X_p(x) = \int_0^x \Phi(x-s)f(s)ds, \tag{3.7.10}$$

In our case, the fundamental matrix is given by $\Phi(x) = e^{Ax}$ and $f$ is continuous so that we can apply both theorems to find the solution.

**Lemma 3.7.3.** *If the matrix $A$ is diagonalizable, then there exists a diagonal matrix $D$ such that,*

$$A = PDP^{-1} \quad \text{and} \quad e^{Ax} = Pe^{Dx}P^{-1}, \tag{3.7.11}$$

*where $P$ and $P^{-1}$ are invertible matrices satisfying $PP^{-1} = I$.*

**Fundamental matrix $\Phi(x)$** The eigenvalues of the matrix $A$ are given by,

$$r_1 = \sqrt{\frac{\lambda}{D_s}} \quad r_2 = -\sqrt{\frac{\lambda}{D_s}}.$$

We have that $A$ is a $(2,2)$ matrix that has exactly 2 distinct eigenvalues, so $A$ is diagonalizable and its diagonal matrix is,

$$D = \begin{pmatrix} r_1 & 0 \\ 0 & r_2 \end{pmatrix},$$

since the associated eigenvectors are as follows,

$$R_1 = \begin{pmatrix} 1 \\ r_1 \end{pmatrix} \quad R_2 = \begin{pmatrix} 1 \\ r_2 \end{pmatrix},$$

then the invertible matrix $P$ is as follow,

$$P = \begin{pmatrix} 1 & 1 \\ r_1 & r_2 \end{pmatrix},$$

thus,

$$\Phi(x) = \begin{pmatrix} \cosh(r_1) & \frac{1}{r_1}\sinh(r_1 x) \\ r_1 \sinh(r_1 x) & \cosh(r_1) \end{pmatrix}. \tag{3.7.12}$$

Now we calculated the fundamental matrix and we already have the form of the particular solution which will lead us to find the general solution in the next paragraph.

**General solution** $X(x)$ The particular solution of the stationary equation is given by:

$$X_p(x) = \int_0^x \Phi(x-s) f(s) ds, \tag{3.7.13}$$

which after some calculations gives rise to,

$$X_p(x) = \begin{pmatrix} -c + c\cosh(r_1 x) \\ r_1 c \sinh(r_1 x) \end{pmatrix}. \tag{3.7.14}$$

Thus we can write the solution as follows,

$$X(x) = X_p(x) + \Phi(x) X_0, \tag{3.7.15}$$

since the solution $X(x) = \begin{pmatrix} u(x) \\ v(x) \end{pmatrix}$ is unique, we have only one $X_0 = \begin{pmatrix} a \\ b \end{pmatrix}$ that verify $u(0) = 0$ and $u(1) = 0$ which come from the boundary conditions of the original model. To find $a$ and $b$, we need to solve the following system,

$$\begin{cases} X_1(0) &= 0, \\ X_1(1) &= 0, \end{cases} \tag{3.7.16}$$

then,

$$\begin{cases} X_{p1}(0) + \Phi_{11}(0)a + \Phi_{12}(0)b &= 0, \\ X_{p1}(1) + \Phi_{11}(1)a + \Phi_{12}(1)b &= 0, \end{cases} \tag{3.7.17}$$

yields to,

$$a = 0; \quad b = \frac{c - c\cosh(r_1)}{\frac{1}{r_1}\sinh(r_1)}. \tag{3.7.18}$$

As a result,

$$X(x) = \begin{pmatrix} -c + c\cosh(r_1 x) + \dfrac{c - c\cosh(r_1)}{\sinh(r_1)}\sinh(r_1 x) \\ cr_1\sinh(r_1 x) + \dfrac{c - c\cosh(r_1)}{\sinh(r_1)} r_1\cosh(r_1 x) \end{pmatrix}. \quad \square$$

Our interest is in the first component of the vector $X$, that is $u(x)$, which leads to the stationary solution $s^*$ of Equation 3.6.1 by setting,

$$s^*(x) = u(x) + c, \tag{3.7.19}$$

As a result,

$$s^*(x) = c\cosh(r_1 x) + \frac{c - c\cosh(r_1)}{\sinh(r_1)}\sinh(r_1 x). \tag{3.7.20}$$

**Theorem 3.7.4.** *If $s(x,t)$ is any solution of Equation (3.6.1), and $s^*(x)$ is the stationary solution, then,*

*i All solutions $s$ tend to $s^*$ as time tends to infinity.*

*ii The stationary solution $s^*$ is stable.*

*Proof.* We want to show that each solution of 3.6.1 tends to the stationary solution $s^*$ as time gets larger. For that, we define,

$$\varepsilon(x,t) = s(x,t) - s^*(x), \tag{3.7.21}$$

which means that $\varepsilon$ verify the following equations,

$$\frac{\partial}{\partial t}\varepsilon = D_s\frac{\partial^2}{\partial x^2}\varepsilon - \lambda\varepsilon, \qquad 0 < x < 1,\ t > 0, \tag{3.7.22}$$

$$\varepsilon(0,t) = \varepsilon(1,t) = 0, \qquad t > 0, \tag{3.7.23}$$

$$\varepsilon(x,0) = \varepsilon_0, \qquad 0 < x < 1, \tag{3.7.24}$$

which can be solved using the separation of variables method to gives rise to,

$$\varepsilon(x,t) = \sum_{n=1}^{\infty}\frac{2\varepsilon_0}{n\pi}(1 - \cos(n\pi))\exp(-n^2\pi^2 D_s t)\exp(-\lambda t)\sin(n\pi x), \tag{3.7.25}$$

from that we can deduce that for $n \in \mathbb{N}^*$ and $t > t_0$,

$$\begin{aligned}
\lim_{t\to\infty}|s - s^*| &= \lim_{t\to\infty}|\varepsilon|, \\
&= \lim_{t\to\infty}|\sum_{n=1}^{\infty}\frac{2\varepsilon_0}{n\pi}(1 - \cos(n\pi))\exp(-n^2\pi^2 D_s t)\exp(-\lambda t)\sin(n\pi x)|, \\
&= \lim_{t\to\infty}|\exp(-\lambda t)\sum_{n=1}^{\infty}\frac{2\varepsilon_0}{n\pi}(1 - \cos(n\pi))\exp(-n^2\pi^2 D_s t)\sin(n\pi x)|, \\
&= \lim_{t\to\infty}|\frac{4\varepsilon_0}{\pi}\exp(-(\lambda + \pi^2 D_s)t)\sum_{n=1}^{\infty}\exp(-(n^2 - 1)\pi^2 D_s t_0)\sin(n\pi x)|, \\
&= 0.
\end{aligned}$$

Thus any solution of Equation 3.6.1 tends to the stationary solution $s^*$. □

The analytical results will be well understood by looking at the numerical simulations of the sensing molecule concentration presented in the following.

## 3.8 Numerical simulation of sensing molecule concentration in time

In this section we present the numerical solution of the reaction-diffusion equation for different time steps. The aim of this is to show that as time gets larger the profile of the solution is the same as the stationary solution.

The left side of Figure 3.3 shows the evolution of sensing molecules distribution profile ($s(x,t)$) as time goes on, starting from the dark green curve until the light green one. This last one is identical to the graph of the stationary solution ($s^*(x)$) on the right side.

Figure 3.4 shows the evolution of sensing molecule concentration in time. The concentration in the free-space starts uniform $s_0 = 2.5$, while the concentration at the surface is lower. As time goes on, the concentration in the free-space decreases, due to the degradation, until it becomes uniform at around $T \approx 3000$, then drop again to smaller values. At the surface, the concentration remains uniform becomes the highest than the free-space concentration at the end.

If we look at the profile of the stationary solution, we see how it is larger near the boundaries where the source is situated. This fact could be explained by the sensing molecules production at the boundaries. If the shape of sensing molecules is always similar to the stationary solution, we get that the direction of bacterial movement in the coupled model will be towards the surface.

We have been modelling each element on its own to have an idea about bacterial behaviour and sensing molecules profile during biofilm initiation. This will help us building the coupled model that will be the interest of the next chapter. Which will be about constructing the mathematical model for both bacteria and sensing molecules, in a three-dimensional space with spherical coordinates. Furthermore, we will introduce bacterial growth to the model and we will perform numerical analysis and discuss the results for both models.

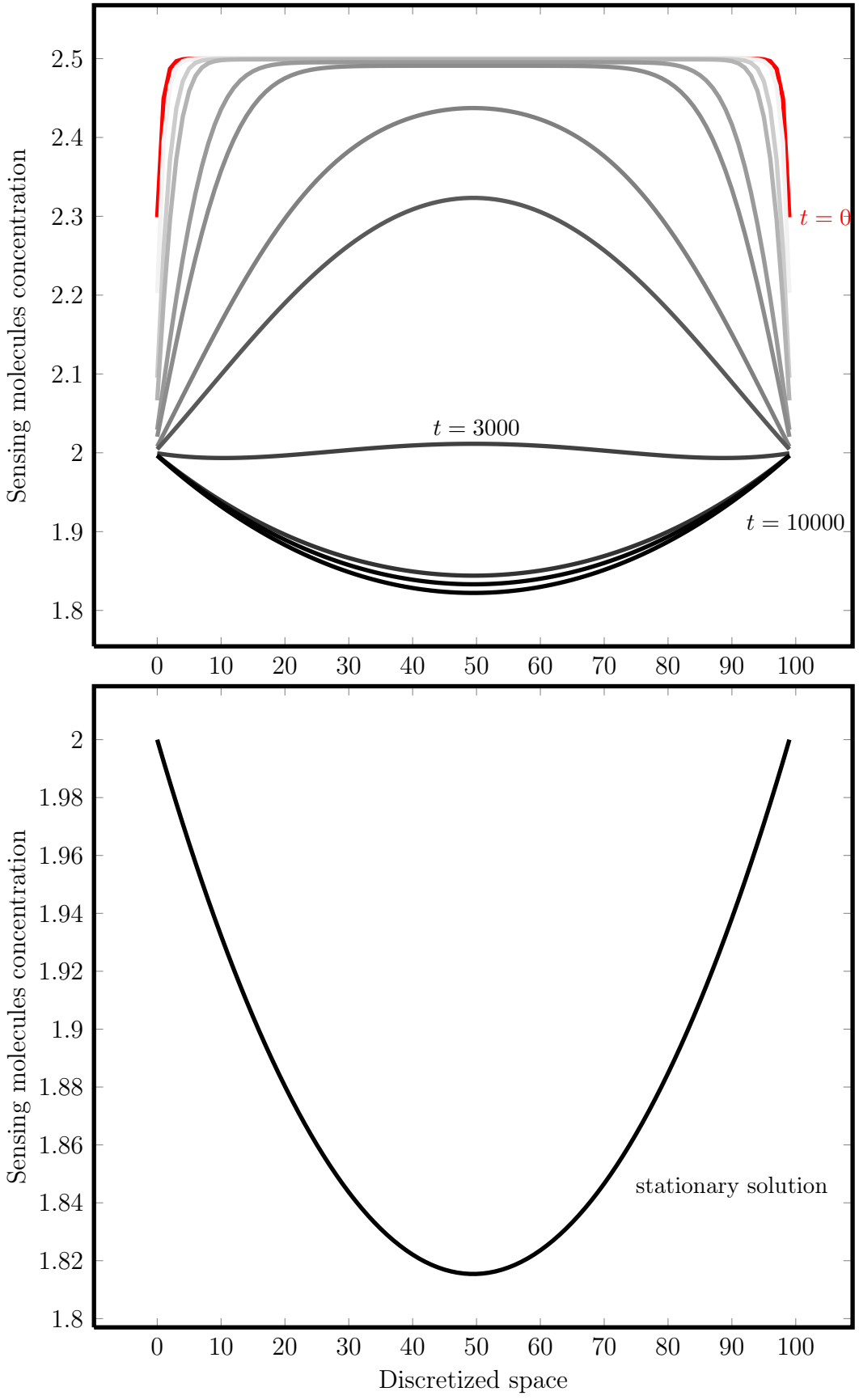


Figure 3.3: Sensing molecules profile in different time steps and the stationary solution distribution. On the top graph we see the sensing molecules profile changes for different time steps. The red curve $T = 0$ represents our initial condition. The rest of time steps range from the light gray curve to the black curve which is identical to the stationary solution in the bottom graph. The parameters used for both simulations are given by: $c = 2$, $\lambda = 0.3$, $D_s = 0.25$ and $s_0 = 2.5$.

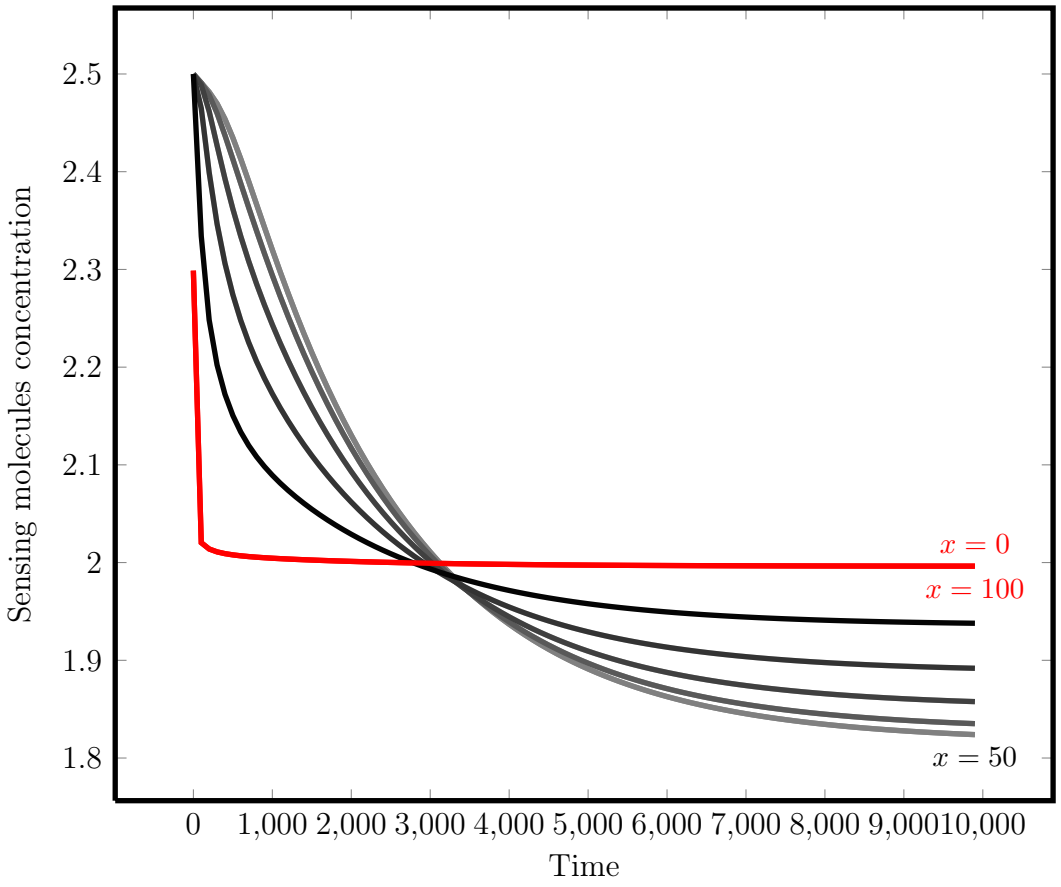


Figure 3.4: The time evolution of sensing molecule concentration, for $c = 2$, $\lambda = 0.3$, $D_s = 0.25$ and $s_0 = 2.5$. The red curve represents the boundaries where the surface is situated. Because of the space symmetry some curves are identical. All the curves cross at around $T \approx 3000$, the concentration there is almost uniform as shown in the top figure of Figure 3.3.

# Chapter 4

# A coupled model of bacterial chemotaxis and sensing molecule diffusion

We have seen how the bacteria move randomly and stick to the surface once they reach the boundaries. But in reality, there are other facts that occur during the bacterial attachment to surfaces and biofilm initiation that need to be considered simultaneously by the model, such as:

- The production of sensing molecules in the free-space and at the surface.
- The diffusion and degradation of sensing molecules over time, and space.
- Bacterial movement towards sensing molecules, this biological behaviour is called chemotaxis [16, 27].

This chapter will be about the coupled model that is of Keller-Segel type [28, 29, 30].

Keller-Segel model is a mathematical model for bacterial chemotaxis. It is composed of two pdes, the first involves bacterial density diffusion, chemotaxis toward the attractant as well as the growth and death. The second concerns the attractant (or the repellent) diffusion degradation and production. The quantities are left in their general form so that they can fit any biological context.

Our model will be presented in a three-dimensional space using Spherical coordinates and will be solved numerically using *Matlab* [31]. The equations will be presented in detail, starting with the main model equations, the boundary conditions which represent our main contribution and the initial conditions. We non-dimensionalize the model equations to remove the units. Then we present and discuss the numerical solutions. Furthermore, bacterial growth will be introduced into the model, the study will be similar to the first model except that here we will just consider a one-dimensional space in

Cartesian coordinates that will be solved numerically using the *Fipy* library in *Python* [32]. The following section is for presenting the main model equations and their description.

## 4.1 Coupling bacterial chemotaxis and sensing molecules production

In this section we will present the coupled model describing bacterial density and sensing molecules concentration. We will define the main equations while the boundary and initial conditions we be presented later on.

We consider a spherical domain, $\Omega$, of center 0 and radius $R$. The parameters used throughout this chapter are presented in Table 4.1.

Table 4.1: State parameters and variables used in this chapter, with their description and units

| Parameter | Description | Unit |
|---|---|---|
| $a$ | Bacterial growth rate | $1/s$ |
| $b, B, B_0$ | Bacterial density | $kg/m^3$ |
| $D_b$ | Bacterial diffusivity | $m^2/s$ |
| $D_s$ | Sensing molecules diffusivity | $m^2/s$ |
| $F$ | Logistic function of bacterial density | $kg/m^3$ |
| $g$ | Proportion of stuck-bacteria per time $t$ | $mol/m^2\ s$ |
| $K$ | Bacterial carrying capacity | $kg/m^3$ |
| $L$ | Non-dimensionalized parameters | No unit |
| $M$ | Non-dimensionalized parameters | No unit |
| $s, S, S_0$ | Sensing molecules concentration | $mol/m^3$ |
| $\alpha$ | Sensing molecules production rate in the free-space | $mol/kg\ s$ |
| $\beta$ | Sensing molecules production rate in the boundaries | $m\ mol/kg\ s$ |
| $\lambda$ | Sensing molecules degradation rate | $1/s$ |
| $\mu$ | Fixed rate of bacterial stickiness | $1/m\ kg$ |
| $\chi$ | Chemotactic coefficient | $m^5/mol\ s$ |
| $\pi$ | Intermediate function | $kg/m^3$ |

The mathematical model does not consider bacterial growth and is presented in Cartesian coordinates by,

$$\frac{\partial b}{\partial t}(\mathbf{x},t) = D_b\frac{\partial^2 b}{\partial \mathbf{x}^2} - \chi\frac{\partial}{\partial \mathbf{x}}(b\frac{\partial s}{\partial \mathbf{x}}), \qquad \text{in } \Omega\times(0,+\infty),$$
$$\frac{\partial s}{\partial t}(\mathbf{x},t) = D_s\frac{\partial^2 s}{\partial \mathbf{x}^2} - \lambda s + \alpha b, \qquad \text{in } \Omega\times(0,+\infty),$$

where all the parameters are constants and presented in Table 4.1 and $\mathbf{x} = (x, y, z) \in \Omega$. The first equation describes bacterial random walk using the diffusion equation. Bacterial chemotaxis is presented by the term $-\frac{\partial J_c}{\partial \mathbf{x}}$, where $J_c$ is the chemotactic flux given by $J_c = \chi b \frac{\partial s}{\partial x}$ with $\chi$ the chemotactic coefficient. In the second equation we describe sensing molecules diffusion, degradation and production.

For simplicity, it is better to write the model in spherical coordinates so that the uniform initial distribution of bacterial density and sensing molecules concentration insure a radial symmetry for our variables, which means that the dependence will be only with respect to the sphere radius. Let us consider the following change of variables

$$b(x, y, z, t) = b(r\sin\theta\cos\varphi, r\sin\theta\sin\varphi, r\cos\theta, t) = B(r, \theta, \varphi, t), \tag{4.1.1}$$
$$s(x, y, z, t) = b(r\sin\theta\cos\varphi, r\sin\theta\sin\varphi, r\cos\theta, t) = S(r, \theta, \varphi, t), \tag{4.1.2}$$

where $r \in [0, R]$, $\theta \in [0, 2\pi]$ and $\varphi \in [0, \pi]$. Because of the radial symmetry we have that,

$$B(r, \theta, \varphi, t) = B(r, t), \tag{4.1.3}$$
$$S(r, \theta, \varphi, t) = S(r, t), \tag{4.1.4}$$

and the model will be written as

$$\frac{\partial B}{\partial t} = \frac{D_b}{r^2}\frac{\partial}{\partial r}(r^2\frac{\partial B}{\partial r}) - \chi(\frac{\partial B}{\partial r}\frac{\partial S}{\partial r} + \frac{B}{r^2}\frac{\partial}{\partial r}(r^2\frac{\partial S}{\partial r})), \qquad 0 < r < R,\ t > 0, \tag{4.1.5}$$

$$\frac{\partial S}{\partial t} = \frac{D_s}{r^2}\frac{\partial}{\partial r}(r^2\frac{\partial S}{\partial r}) - \lambda S + \alpha B, \qquad 0 < r < R,\ t > 0. \tag{4.1.6}$$

Once our main equations are defined we should give the appropriate boundary and initial conditions to the model. This will be the subject of the next section.

## 4.2 Initial and boundary conditions

This section concerns bacterial density and sensing molecules dynamics at the surface. Bacteria are assumed to be stuck once the surface is reached, which means that we will use absorbing boundary conditions. While for sensing molecules we have more than one behaviour happening at the same time. They diffuse, get produced and they degrade at the surface. To express this mathematically we need to build our own boundary conditions, and this is what we explain in this section.

**At $r = 0$:** Starting from a uniform distribution for both bacteria and sensing molecules, we have that our variables are radially symmetric which insure that the flux coming in at $r = 0$ is the same as the one going out. For that we have zero-Neumann boundary conditions at $r = 0$ given by,

$$\frac{\partial B}{\partial r}(0,t) = 0, \qquad t > 0, \tag{4.2.1}$$

$$\frac{\partial S}{\partial r}(0,t) = 0, \qquad t > 0. \tag{4.2.2}$$

**At $r = R$:** For bacteria we are going to use zero-Dirichlet boundary conditions at $r = R$. Assuming that the surface where bacteria get stuck is actually the sphere surface, i.e.

$$B(R,t) = 0, \quad t > 0. \tag{4.2.3}$$

For sensing molecules, the boundary condition at $r = R$ is much more complicated, since there are many facts happening simultaneously. At the surface, sensing molecules degrade, diffuse and are produced by both free-bacteria and stuck-bacteria. To distinguish between the two we will consider sensing production by free-bacteria as their growth and stuck-bacteria as a source.

To derive the equation at the boundaries we need to use the conservation equation, which needs to be defined in a given volume. In our case we take a spherical cap $V$ to be our domain. $V$ is defined as follows,

$$V = \{(r,\theta,\varphi),\ R-\Delta r \le r \le R; \Theta-\Delta\theta \le \theta \le \Theta+\Delta\theta; \Phi-\Delta\varphi \le \varphi \le \Phi+\Delta\varphi\},$$

so that after tending $\Delta r$, $\Delta\theta$ and $\Delta\varphi$ to zero, we obtain the equation of sensing molecules at the point $(R,\theta,\varphi)$ which will be the same for all the points on the sphere surface. The conservation equation gives,

$$\underbrace{\frac{\partial}{\partial t}\int_V S dV}_{\bigstar} = \underbrace{\underbrace{-\int_{\partial V} J\partial V}_{\text{Sensing chemicals flux}} + \underbrace{\int_V f(S,B)dV}_{\text{Growth and degradation}} + \underbrace{\int_{\partial V} g(t)\partial V}_{\text{Source at surface}}}_{\spadesuit}, \tag{4.2.4}$$

where,

$$\begin{cases} \partial V = S_{base} + S_{lateral} + S_{top}, \\ f(S,B) = -\lambda S + \alpha B, \\ g(t) = \beta B_{wall}(t) = \beta(B_0 - \int_0^R B(r,t)dr). \end{cases}$$

The $S_{base}$ and $S_{top}$ are the base and top surfaces of the spherical cap, and the $S_{lateral}$ are the four surfaces around the spherical cap defined by $\theta$ and $\varphi$. Because of the radial symmetry, the fluxes coming into the volume $V$ through

the lateral surfaces are equal to the fluxes going out, so that they cancel each other. On left side, the quantity noted by ★ leads to,

$$\begin{aligned}\frac{\partial}{\partial t}\int_V S dV &= \int_V \frac{\partial S}{\partial t} dV, \\ &= \int_V D_s \frac{\partial^2 S}{\partial r^2} dV + \int_V f(S,B) dV,\end{aligned}$$

using the Divergence theorem we obtain,

$$\begin{aligned}\int_V D_s \frac{\partial^2 S}{\partial r^2} dV + \int_V f(S,B) dV &= \int_{\partial V} D_s \frac{\partial S}{\partial r} \partial V + \int_V f(S,B) dV, \\ &= \int_{S_{base}} D_s \frac{\partial S}{\partial r} dS + \int_{S_{lateral}} D_s \frac{\partial S}{\partial r} dS + \int_{S_{top}} D_s \frac{\partial S}{\partial r} dS \\ &+ \int_V f(S,B) dV,\end{aligned}$$

since the lateral fluxes cancel each other, the final expression is given by,

$$\frac{\partial}{\partial t}\int_V S dV = \int_{S_{base}} D_s \frac{\partial S}{\partial r} dS + \int_{S_{top}} D_s \frac{\partial S}{\partial r} dS + \int_V f(S,B) dV. \qquad (4.2.5)$$

On the right side, the quantity noted by ♠ gives rise to,

$$\begin{aligned}\underbrace{-\int_{\partial V} J \partial V}_{Sensing\ chemicals\ flux} &= -\{\int_{S_{base}} J dS + \int_{S_{lateral}} J dS + \int_{S_{top}} J dS\}, \\ \underbrace{\int_V f(S,B) dV}_{Growth\ and\ degradation} &= \int_V f(S,B) dV, \\ \underbrace{\int_{\partial V} g(t) \partial V}_{Source\ at\ surface} &= \int_{S_{base}} g(t) dS + \int_{S_{lateral}} g(t) dS + \int_{S_{top}} g(t) dS,\end{aligned}$$

we only have a source from the stuck-bacteria which make lateral and base sources equal to zero, again the lateral fluxes cancel each other and there is no flux coming from the top surface, so that we can write,

$$\begin{aligned}\underbrace{-\int_{\partial V} J \partial V}_{Sensing\ chemicals\ flux} &= -\int_{S_{base}} J dS = \int_{S_{base}} D_s \frac{\partial S}{\partial r} dS, \\ \underbrace{\int_V f(S,B) dV}_{Growth\ and\ degradation} &= \int_V f(S,B) dV, \\ \underbrace{\int_{\partial V} g(t) \partial V}_{Source\ at\ surface} &= \int_{S_{top}} g(t) dS,\end{aligned}$$

which is equivalent to,

$$\underbrace{-\int_{\partial V} J\partial V}_{\text{Sensing chemicals flux}} + \underbrace{\int_V f(S,B)dV}_{\text{Growth and degradation}} + \underbrace{\int_{\partial V} g(t)\partial V}_{\text{Source at surface}} = \int_{S_{base}} D_s\frac{\partial S}{\partial r}dS + \int_V f(S,B)dV + \int_{S_{top}} g(t)dS,$$

together with Equation (4.2.5), let Equation (4.2.4) becomes,

$$\int_{S_{base}} D_s\frac{\partial S}{\partial r}dS+\int_{S_{top}} D_s\frac{\partial S}{\partial r}dS+\int_V f(S,B)dV = \int_{S_{base}} D_s\frac{\partial S}{\partial r}dS+\int_V f(S,B)dV+\int_{S_{top}} g(t)dS,$$

thus,

$$\int_{S_{top}} D_s\frac{\partial S}{\partial r}dS = \int_{S_{top}} g(t)dS, \tag{4.2.6}$$

which we integrate in spherical coordinates as follows,

$$\begin{aligned}
&\int_{S_{top}} D_s\frac{\partial S}{\partial r}dS = \int_{S_{top}} g(t)dS,\\
&\Rightarrow D_s\int_{\varphi-\Delta\varphi}^{\varphi+\Delta\varphi}\int_{\theta-\Delta\theta}^{\theta+\Delta\theta}\frac{\partial S}{\partial r}r^2\sin\theta d\theta d\varphi = \int_{\varphi-\Delta\varphi}^{\varphi+\Delta\varphi}\int_{\theta-\Delta\theta}^{\theta+\Delta\theta} g(t)r^2\sin\theta d\theta d\varphi,\\
&\Rightarrow D_s\frac{\partial S}{\partial r}r^2 2\Delta\varphi(-2\sin\theta\sin\Delta\theta) = r^2 g(t)2\Delta\varphi(-2\sin\theta\sin\Delta\theta)
\end{aligned}$$

thus,

$$D_s\frac{\partial S}{\partial r}(R,t) - \beta(B_0 - \int_0^R B(r,t)dr) = 0, \quad t>0. \tag{4.2.7}$$

This type of boundary conditions is called Robin boundary conditions. Our boundary conditions at $r=R$ are summarized as follows,

$$B(R,t) = 0, \quad t>0, \tag{4.2.8}$$

$$D_s\frac{\partial S}{\partial r}(R,t) - \beta(B_0 - \int_0^R B(r,t)dr) = 0, \quad t>0. \tag{4.2.9}$$

To explain the biological interpretation of Equation (4.2.9) we consider the following,

$$D_s\frac{\partial S}{\partial r}(R,t) - \beta(B_0 - \int_0^R B(r,t)dr) = 0, \tag{4.2.10}$$

$$\Rightarrow \quad \frac{\partial S}{\partial r}(R,t) = \frac{\beta}{D_s}(B_0 - \int_0^R B(r,t)dr), \tag{4.2.11}$$

$$\Rightarrow \quad \frac{S(R,t)-S(R-\Delta r,t)}{\Delta r} = \frac{\beta}{D_s}(B_0 - \int_0^R B(r,t)dr), \tag{4.2.12}$$

$$\Rightarrow \quad S(R,t)-S(R-\Delta r,t) = \frac{\beta}{D_s}\Delta r(B_0 - \int_0^R B(r,t)dr). \tag{4.2.13}$$

Depending on the sensing molecules diffusivity $D_s$ and the production rate $\beta$ we have four cases:

**When** $\beta increases \Leftrightarrow S(R,t) \gg S(R-\Delta r,t)$**:** It means that we have high production of sensing molecules at the surface so that the sensing molecules concentration at the surface is much higher than in the free-space.

**When** $\beta decreases \Leftrightarrow S(R,t) \approx S(R-\Delta r,t)$**:** Here the production is very low so that the concentration is approximately the same in the free-space and at the surface.

**When** $D_s increases \Leftrightarrow S(R,t) \approx S(R-\Delta r,t)$**:** When the diffusivity is high, the sensing molecules move very fast and are able to displace from the surface where they are produced to the free-space.

**When** $D_s decreases \Leftrightarrow S(R,t) \gg S(R-\Delta r,t)$**:** When diffusivity is small the movement of sensing molecules is very slow which explain that they spend more time at the surface before moving to the free-space.

For initial conditions, we assume that the bacteria start in a uniform distribution with a very low amount of sensing molecules present, so we have,

$$\begin{aligned} B(r,0) &= B_0, & 0 < r < R, \\ S(r,0) &= S_0, & 0 < r < R, \end{aligned}$$

where $B_0$ and $S_0$ are constants defined in Table 4.1.

## 4.3 Non-dimensionalization

The mathematical model involves measured parameters and variables, the reason why it should be non-dimensionalized before being studied. First, to remove the units and second to reduce the number of parameters used. To non-dimensionalize Equations (4.1.5) and (4.1.6), we introduce the non-dimensional variables $B^*$, $S^*$, $x^*$, and $t^*$ defined by,

$$t = \omega t^*, \quad B = B_0 B^*, \quad S = S_0 S^*, \quad r = R r^*. \tag{4.3.1}$$

In terms of these variables Equations (4.1.5) and (4.1.6) become,

$$\frac{R^2}{D_b \omega}\frac{\partial B^*}{\partial t^*} = \frac{1}{r^{*2}}\frac{\partial}{\partial r^*}(r^{*2}\frac{\partial B^*}{\partial r^*}) - \frac{\chi S_0}{D_b}(\frac{\partial B^*}{\partial r^*}\frac{\partial S^*}{\partial r^*} + \frac{B^*}{r^{*2}}\frac{\partial}{\partial r^*}(r^{*2}\frac{\partial S^*}{\partial r^*})), \tag{4.3.2}$$

$$\frac{1}{\lambda\omega}\frac{\partial S^*}{\partial t^*} = \frac{D_s}{R^2\lambda}\frac{1}{r^{*2}}\frac{\partial}{\partial r^*}(r^{*2}\frac{\partial S^*}{\partial r^*}) - S^* + \frac{\alpha B_0}{\lambda S_0}B^*, \tag{4.3.3}$$

with boundary conditions given as,

$$\frac{\partial B^*}{\partial r^*}(0,t^*) = \frac{\partial S^*}{\partial r^*}(0,t^*) = 0, \tag{4.3.4}$$

$$B^*(R,t^*) = 0, \quad \frac{\partial S^*}{\partial r^*}(R,t^*) = -\frac{R\beta\chi}{D_s D_b}B_0 + \frac{\beta\lambda}{D_s\alpha}\int_0^R B^*(r^*,t^*)dr^*, \tag{4.3.5}$$

and initial conditions,

$$B^*(r^*,0) = \frac{B_0\alpha\chi}{D_b\lambda} = B_0^*, \tag{4.3.6}$$

$$S^*(r^*,0) = \frac{S_0\chi}{D_b} = S_0^*. \tag{4.3.7}$$

This form suggests the choices,

$$\omega = \frac{D_s}{D_b\lambda}, \quad R = \sqrt{\frac{D_s}{\lambda}}, \quad S_0 = \frac{D_b}{\chi}, \quad B_0 = \frac{D_b\lambda}{\alpha\chi}. \tag{4.3.8}$$

Furthermore, we obtain the three non-dimensional parameters $\tau$, $L$ and $M$, defined by,

$$\tau \equiv \frac{D_b}{D_s}, \quad L \equiv \frac{R\beta\chi B_0}{D_s D_b}, \quad M \equiv \frac{\beta\lambda}{D_s\alpha}. \tag{4.3.9}$$

Using these new variables, on dropping the asterisks for simplicity, we obtain the non-dimensionalized equations,

$$\begin{cases} \dfrac{\partial B}{\partial t} = \dfrac{1}{r^2}\dfrac{\partial}{\partial r}(r^2\dfrac{\partial B}{\partial r}) - (\dfrac{\partial B}{\partial r}\dfrac{\partial S}{\partial r} + \dfrac{B}{r^2}\dfrac{\partial}{\partial r}(r^2\dfrac{\partial S}{\partial r})), \\ \tau\dfrac{\partial S}{\partial t} = \dfrac{1}{r^2}\dfrac{\partial}{\partial r}(r^2\dfrac{\partial S}{\partial r}) - S + B, \\ \dfrac{\partial B}{\partial r}(0,t) = \dfrac{\partial S}{\partial r}(0,t) = 0, \\ B(R,t) = 0, \quad \dfrac{\partial S}{\partial r}(R,t) - (L - M\displaystyle\int_0^R B(r,t)dr) = 0, \\ B(r,0) = B_0, \\ S(r,0) = S_0. \end{cases} \tag{4.3.10}$$

Our model is now ready to be studied, in the next section we will solve the mathematical model numerically and present the obtained results.

## 4.4 Numerical simulation of the non-dimensionalized coupled model

The model presented in this chapter involves both bacteria and the presence of sensing molecules which direct bacterial movement, this phenomenon is known

as chemotaxis. The presence of chemotaxis in the model makes it a Keller-Segel type model that is difficult to study analytically. This is the reason why we choose to study the model numerically. For that we non-dimensionalize the equations to remove the units and reduce the number of parameters and then implement the equations either by using *Matlab* or *Python*. Finally, we present the obtained results.

Even numerically, it is not easy to study Problem (4.3.10). The term $1/r^2$ represents a singularity problem when $r$ is very small. Fortunately, *Matlab* can deal with such problems using the function *Pdepe* that solves initial-boundary value problem for system of parabolic-elliptic partial differential equations, so implementing the main equations is not a problem until now, the big challenge comes when implementing the boundary equation of sensing molecules, namely,

$$\frac{\partial S}{\partial r}(R,t) - (L - M\int_0^R B(r,t)dr) = 0, \tag{4.4.1}$$

where the equation needs to be defined at a specified value of $r$, while the integral $\int_0^R B(r,t)dr$ needed to be calculated over all the interval of $r$-values, i.e. $[0,R]$. To solve this problem we call an intermediate function $\pi(r,t)$ that does not appear at any of our equations except at the boundary condition of sensing molecules when $r = R$. For that, we need to build the function $\pi$ in order for to verify,

$$\pi(R,t) = \int_0^R B(r,t)dr. \tag{4.4.2}$$

This means that the intermediate function $\pi(R,t)$ and the value of $\int_0^R B(r,t)dr$ are the same at the boundary. Since the integral value is the same as the value of $\pi$ at the points when $r = R$, there is no need to express the integral in the boundary conditions. We will rather use the value of $\pi$ which result from solving the following problem,

$$\begin{cases} D\dfrac{\partial \pi}{\partial t} = \dfrac{\partial^2 \pi}{\partial r^2} - \dfrac{\partial B}{\partial r}, \quad 0 < r < R,\ t > 0, \\ \pi(0,t) = 0, \quad \dfrac{\partial \pi}{\partial r}(R,t) - B(R,t) = 0, \quad t > 0, \\ \pi(r,0) = rB_0, \quad 0 < r < R. \end{cases} \tag{4.4.3}$$

We consider that $D = 0$ and we easily solve Problem (4.4.3) to get,

$$\pi(r,t) = \int_0^r B(x,t)dx, \tag{4.4.4}$$

which will be used in the numerical simulation instead of the complication we had. The obtained numerical results are shown in Figure 4.1 and Figure 4.2.

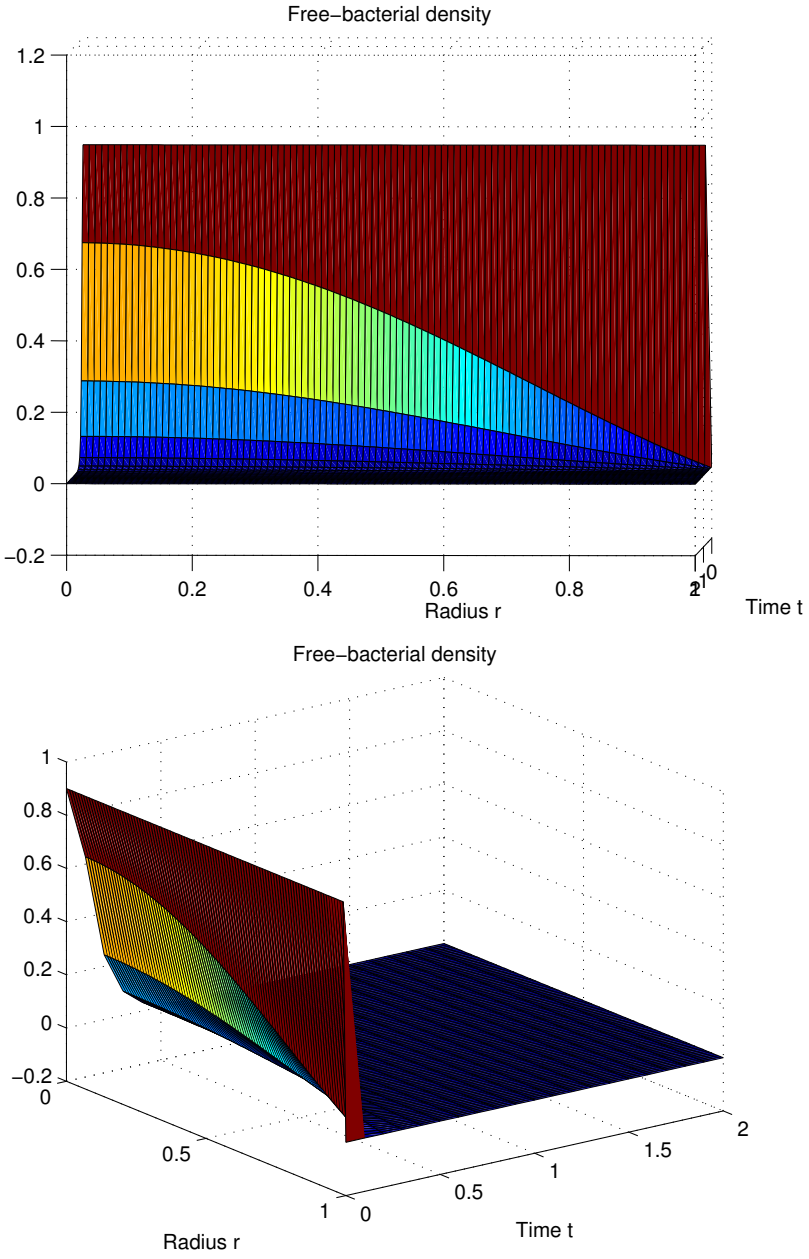


Figure 4.1: Two views of free-bacterial density distribution profile in space, as well as the density evolution in time, for $R = 1$, $\tau = 2.5$, $L = 0.75$ and $M = 0.7$. The top graph shows that bacterial distribution starts uniform and become of a Gaussian distribution shape to end up uniform that is almost zero everywhere. The bottom plot shows the free-bacterial density evolution over time which is the total density at the starting point and tends to zero as more bacteria stick to the surface with time.

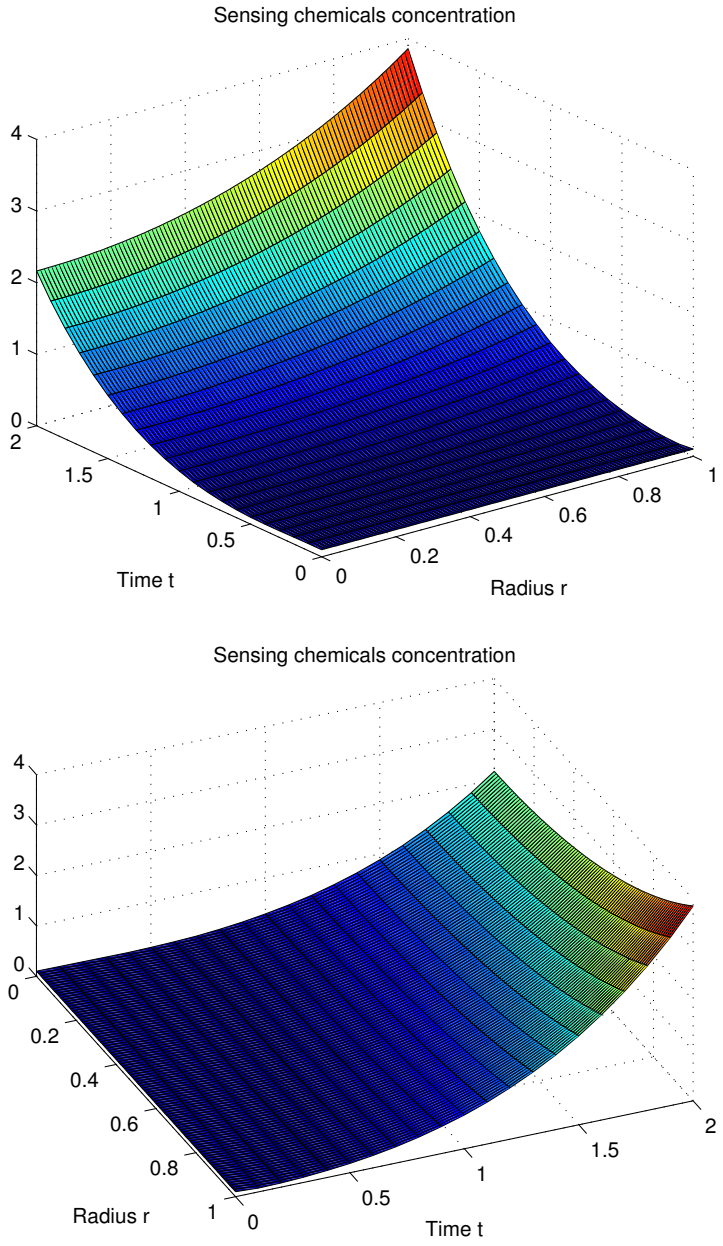


Figure 4.2: Sensing molecule distribution profile in space (top graph) and evolution in time (bottom graph), for $R = 1$, $\tau = 2.5$, $L = 0.75$ and $M = 0.7$. The top graph shows that the sensing molecules distribution starts very low then increases everywhere except that it is much higher near the surface. For the bottom graph, it shows that the sensing molecules concentration increases exponentially with time.

Figure 4.1 shows that bacterial density distribution is changing its curve over time, the peak is decreasing and the shape is changing from uniform at the beginning, to a Gaussian shape then to a uniform almost equal to zero. The total density is decreasing over time and tending to zero. For sensing molecules, we see in Figure 4.2 that the concentration profile is starting at zero and then getting larger, especially near the boundaries.

The biological interpretation of these results is that bacterial distribution profile changes as far as bacteria get stuck to the surface, it becomes of Gaussian shape when sensing molecules concentration is still relatively small. Once the amount of bacteria stuck is large, more sensing molecules are produced at the surface which leads to more attracted bacteria the fact that explain the passage from Gaussian shape to a uniform again but this time with a decrease in the total bacterial density which means that the majority of the population is at the surface and only a negligible amount remain in the free-space.

To improve our model we will introduce bacterial growth. The biological assumptions will remain the same except that the total population of bacteria will change with time in the free-space and at the surface. The effect that the growth has on the models equation will be explained in the next section.

## 4.5 Adding growth to the coupled model of chemotaxis

In this part, the model will be presented in one dimensional space $[0, 1]$ and we will consider a growing population of bacteria. The biological assumption added to the model says that bacteria is performing a logistic growth in the free-space and at the surface, for that the equations will have the form,

$$\begin{cases} \dfrac{\partial b}{\partial t} = D_b \dfrac{\partial^2 b}{\partial x^2} - \chi \dfrac{\partial}{\partial x}\left(b \dfrac{\partial s}{\partial x}\right) + abF(b), & 0 < x < 1,\ t > 0, \\ \dfrac{\partial s}{\partial t} = D_s \dfrac{\partial^2 s}{\partial x^2} - \lambda s + \alpha b, & 0 < x < 1,\ t > 0, \\ \dfrac{db_{wall}}{dt} = a b_{wall} F(b_{wall}) + \mu g(t), & 0 < x < 1,\ t > 0, \\ b(0,t) = b(1,t) = 0, & t > 0, \\ D_s \dfrac{\partial s}{\partial x}(0,t) + \beta b_{wall}(t) = 0, & t > 0, \\ D_s \dfrac{\partial s}{\partial x}(1,t) - \beta b_{wall}(t) = 0, & t > 0, \\ b(x,0) = b_0,\ s(x,0) = s_0,\ b_{wall}(0) = b_{wall0}, & 0 < x < 1, \end{cases} \tag{4.5.1}$$

where $a$, $K$ and $\mu$ are defined in Table 4.1, while $g(t)$ is the proportion of bacteria stuck to the surface at each time $t$ and for logistic growth we have $F(b) = 1 - b/K$. Since we are dealing with a growing population of bacteria,

we remark that the expression of bacterial density at the surface is no more the total density minus the stuck-bacteria, we rather need to solve an ordinary differential equation to obtain bacterial density at the surface. Moreover, we derive $g(t)$ from the conservation equation of the total bacterial density in the free-space that is,

$$\begin{aligned}
&\frac{\partial}{\partial t}\int_0^1 b dx = \underbrace{a\int_0^1 b(1-b/K)dx}_{Bacterial\ growth} - \underbrace{g(t)}_{Stuck-Bacteria},\\
&\Rightarrow \int_0^1 \frac{\partial b}{\partial t}dx = a\int_0^1 b(1-b/K)dx - g(t),\\
&\Rightarrow \int_0^1 \{D_b\frac{\partial^2 b}{\partial x^2} - \chi\frac{\partial}{\partial x}(b\frac{\partial s}{\partial x}) + ab(1-b/K)\}dx = a\int_0^1 b(1-b/K)dx - g(t),\\
&\Rightarrow \left[D_b\frac{\partial b}{\partial x} - \chi(b\frac{\partial s}{\partial x})\right]_{x=0}^{x=1} + \int_0^1 ab(1-b/K)dx = a\int_0^1 b(1-b/K)dx - g(t),\\
&\Rightarrow D_b\left[\frac{\partial b}{\partial x}(1,t) - \frac{\partial b}{\partial x}(0,t)\right] = -g(t),
\end{aligned}$$

since our variables are symmetric we have that $\frac{\partial b}{\partial x}(1,t) = -\frac{\partial b}{\partial x}(0,t)$, which means that,

$$g(t) = 2D_b\frac{\partial b}{\partial x}(1,t). \tag{4.5.2}$$

As in Section 4.3, we need to non-dimensionalize the model in order to determine the relative importance of the mechanisms involved. We denote non-dimensional quantities with hats and we rescale the variables using,

$$t = t^*/a,\ x = x^*/a,\ b = Kb^*,\ s = \frac{\alpha K}{a}s^*,\ b_{wall} = Kb^*_{wall},\ F(b) = F^*(b^*);$$

we note that $F^*(b^*) = 1-b^*$, which means that after the non-dimensionalization the carrying capacity of bacteria becomes 1, and the model equations become,

$$\begin{cases}
\frac{\partial b^*}{\partial t^*} = D_b^*\frac{\partial^2 b^*}{\partial x^{*2}} - \chi^*\frac{\partial}{\partial x^*}(b^*\frac{\partial s^*}{\partial x^*}) + b^*F^*(b^*), & 0<x^*<1,\ t^*>0,\\
\frac{\partial s^*}{\partial t^*} = D_s^*\frac{\partial^2 s^*}{\partial x^{*2}} - \lambda^* s^* + b^*, & 0<x^*<1,\ t^*>0,\\
\frac{db^*_{wall}}{dt^*} = b^*_{wall}F^*(b^*_{wall}) + \mu^*\frac{\partial b^*}{\partial x^*}(1,t^*), & 0<x^*<1,\ t^*>0,\\
b^*(0,t^*) = b^*(1,t^*) = 0, & t^*>0,\\
\frac{\partial s^*}{\partial x^*}(0,t^*) + \beta^* b^*_{wall}(t^*) = 0, & t^*>0,\\
\frac{\partial s^*}{\partial x^*}(1,t^*) - \beta^* b^*_{wall}(t^*) = 0, & t^*>0,\\
b^*(x^*,0) = b^*_0,\ s^*(x^*,0) = s^*_0,\ b^*_{wall}(0) = b^*_{wall0}, & 0<x^*<1,
\end{cases} \tag{4.5.3}$$

where $D_s^* = aD_s$, $D_b^* = aD_b$, $\chi^* = \alpha K\chi$, $\lambda^* = \lambda/a$, $\mu^* = 2\mu D_b$ and $\beta^* = \beta/\alpha D_s$.

Furthermore, we drop the hats for simplicity and we implement the model. We use *FiPy* which is an object oriented, partial differential equation (PDE) solver, written in *Python*. *Fipy* uses the Finite Volume Method (FVM), a method for writing PDE's in the form of algebraic equations [33]. The name "Finite Volume" refers to the small volume surrounding each node point on a mesh. The method uses Gauss' Divergence Theorem to convert volume integrals in a partial differential equation that contains a divergence term to a surface integrals. Then the terms are evaluated as fluxes at the surfaces of each finite volume. The method is easily formulated to allow for unstructured meshes and it is conservative, since the flux entering the volume is identical to the one leaving the adjacent volume.

In one-dimensional space, the finite volume method is based on subdividing the spatial domain into intervals (the " finite volume" also called *grid cells*) and finding an approximation to the integral of the functions over each of these volumes. In each time step we update these values using approximations to the flux through the endpoints of the intervals.

Using *Fipy* we implement the mathematical model for $\lambda = 0.2$, $\mu = 0.3$, $\chi = 0.9$, $\beta = 0.5$, $D_s = 0.5$ and $D_b = 0.25$. In Figure 4.3 we see the sensing molecules concentration profile where in Figure 4.4 we have the bacterial density in the free-space and at the surface as well as sensing molecules concentration evolution in time.

Even with a growing population of bacteria, the density is almost zero as time gets larger so that the bacteria accumulates at the surface to start growing as a biofilm. This fact also explains the shape that takes sensing molecules concentration at the final time step, as we can see in Figure 4.3 the concentration is much higher near the surface because of the high production near the surface and the low production in the free-space.

Figure 4.4 shows that free-bacterial density takes a long time before dropping to zero. This means that bacterial growth has kept bacteria in the free-space longer. While stuck-bacteria also grow so that their density is increasing but still bellow the carrying capacity. Being produced by both free and stuck-bacteria, sensing molecules concentration is exponentially increasing. This would attract more bacteria to the surface and facilitate biofilm initiation.

In the following chapter, the work done in this thesis will be discussed and criticized. The results obtained will be presented in details. Then, we will end the chapter by some possible extensions of our model as well as some other perspectives.

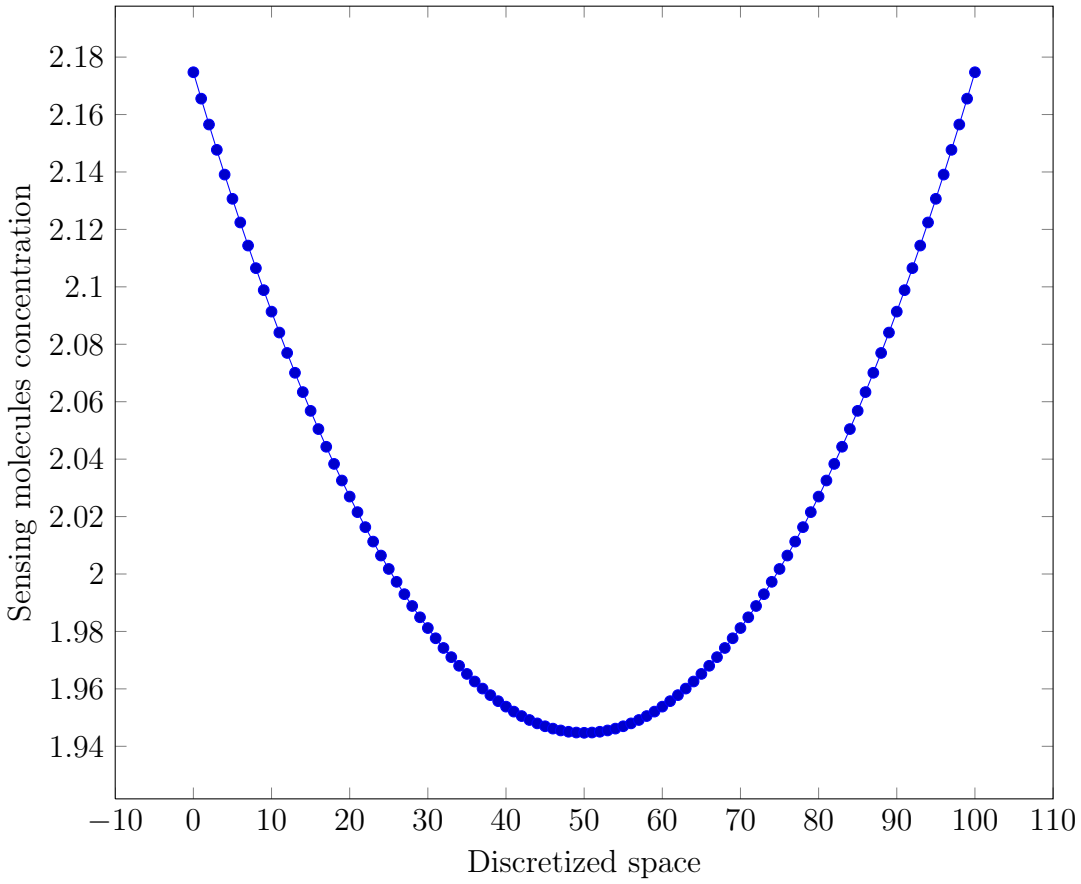


Figure 4.3: sensing molecules distribution profile in a discretized interval $[0, 1]$, at the final time step $T = 40000$. The simulation started with a very low amount of sensing molecules present in the free-space $s_0 = 0.01$ uniformly distributed.

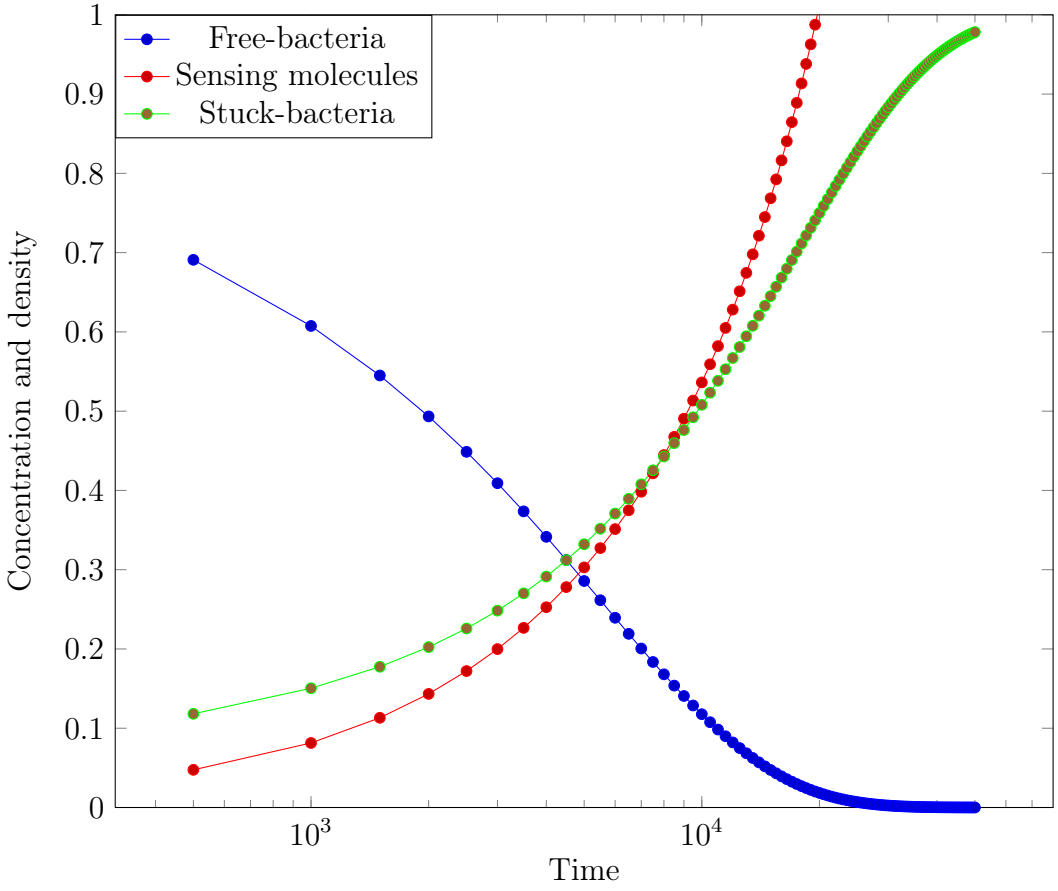


Figure 4.4: the evolution of bacterial density in the free-space and at the surface with the sensing molecules concentration. We start with bacteria in the free-space that stick to the surface so that the density in the free-space drop to zero and the density at the surface increases until it reaches the carrying capacity, for sensing molecules they are produced by both free and stuck bacteria thus they increase exponentially.

# Chapter 5

# Discussion, context and conclusion

In this chapter, we start by a summary of the work we perform throughout this thesis. In the second section, we critically discuss our results and give some perspectives. Then, we end with a small conclusion.

## 5.1 Summary of results

Chapter 2 describes the existing different ways of modelling bacterial biofilm, which vary from computational models, to continuum or discrete models. The aim of presenting these models, is to show the diversity of biofilm mathematical models that motivate us to find another way of modelling biofilm.

By looking at the biological description of bacterial attachment to surfaces and biofilm initiation, we succeeded to build the mathematical model describing this phenomenon. In Chapter 3, we started presenting our own work which consists of three mathematical models. The first model describes bacterial movement and attachment without including the presence of sensing molecules. The second model is about sensing molecules dynamics, production and degradation. While the third model that is presented in Chapter 4, includes both bacteria and sensing molecules interacting with each other.

The model describing bacterial movement uses the Fokker-Planck equation without drift that describes the Brownian motion of bacterial population. We choose a uniform initial distribution, and boundary conditions that represent bacterial stickiness. Using the separation of variable method and the superposition principle, we solve the equation analytically. A steady-state analysis was also performed to show that the total bacterial density tends to the stable trivial equilibrium. This indicates that as time goes on the bacterial density is almost zero everywhere. We plot the results and see the evolution of both bacterial densities, at the surface and in the free-space over time. The bacterial density at the free-space tends to zero and the bacterial density at the boundaries tends to the total density, which is similar to the analytical results.

Before moving to the coupled model, we model sensing molecules on their

own. The model is a reaction-diffusion equation with a fixed source at the boundaries. The equation describes sensing molecules movement, production and degradation. A steady-state analysis was performed showing that all solutions tend to a stable stationary solution obtained analytically. This result explains that however the sensing molecules distribution starts, it will always end up identical to the stationary solution. This result was emphasized by the numerical simulation of sensing molecules concentration compared to the stationary solution plot.

Finally, in Chapter 4, we consider a high bacterial population, so that the amount of sensing molecules produced by the bacteria to sense their proximity to the surfaces is significant. We have a coupled mathematical model of Keller-Segel type, representing bacterial density and sensing molecules concentration, in three-dimensional space. Bacteria perform a random movement directed by the sensing molecules attractant. The sensing molecules diffuse, degrade and are produced by both bacterial populations, at the surface and in the free-space. We started by a fixed population of bacteria, then we added bacterial growth to our model later on. It was very challenging to define the boundary equations for sensing molecules, since they get produced at the surface, they degrade and then diffuse and none of these behaviours could be neglected in the equation describing the boundary conditions. The model's equations are very complicated to be studied analytically, so one way of studying this model is through numerical analysis. For that, we non-dimensionalize the equations to get rid of the units and reduce the number of parameters. We use *Matlab* for numerical results which show the sensing molecules distribution and bacterial density profile in space, as well as their evolution over time. A similar analysis was performed for the model including bacterial growth.

## 5.2 Discussion and perspectives

Biofilm study is among the interesting topics in mathematical modelling, because of its importance in many industrial processes. In our model we showed the importance of the first stages of biofilm formation. We started by describing the biology of these phases before presenting the mathematical model. These stages are very important for constructing a biofilm and this was our main motivation to build our model. Other modellers choose to model either the final shape of biofilms, the biofilm growth or the interactions between biofilm and the surrounding environment. These phenomena occurs within the third and forth stages of biofilm, that are the the first and second biofilm maturation as given in [8].

Our results show that bacterial density starts as a uniform distribution within a well defined medium, then search for surfaces to stick to it. Since we place the surface at the boundaries, we remark that as bacteria get stuck, the shape of bacterial density distribution changes to a Gaussian before to

return back to a uniform, this time almost zero everywhere. This means that the majority of bacteria are stuck to the surface, the fact that agrees with the biological description the nature of bacterial life given in [21]. It says that the free-living bacteria look for, whether a living or non-living surface to stick before aggregating as a biofilm. This explained the result showing the evolution of the total bacterial density in time that tends to zero as time gets larger meaning that the density distribution is almost zero everywhere.

It was also mentioned in [21] how the bacteria search for surfaces. They use sensing molecules to sense their proximity to the surface before they attach to it. This fact was also included in our model as chemotaxis [8], which means that bacterial movement is a random walk directed by the sensing molecules attractant. For sensing molecules, our results show that their concentration gets higher near the surface as time goes on. Since the sensing molecules are produced by bacteria and that bacterial density gets larger at the surface then the production at the surface is much higher than the production in the free-space. The presence of highly concentrated sensing molecules near the surface is essential for biofilm construction. The bacteria will move towards the high concentration of sensing molecules, get stuck to the surface and then keep producing the sensing molecules to attract other bacteria to join the aggregation. This explained the increasing sensing molecules concentration with time obtained by showing sensing molecules concentration evolution in time.

Our work gives rise to results that agree with the biological description of the early stages of biofilm formation. However, our model do not include some important elements that participate in building biofilm such as bacterial nutrients and temperature. Of course including such elements will make the model more realistic but also more complex to be studied, even for a numerical study. But still, a more relevant work would be to do real experiments for one or more bacterial species and look at their biofilm initiation then compare the experimental results to the mathematical model, after that we will be able to manipulate bacterial behaviour through mathematical studies.

For our model to be more useful in a medical or industrial point of view, we should extend it to study the inhibition of the bacterial attachment to surfaces. This model will help us to manipulate biofilm formation depending on our needs, either to accelerate it formation when it is beneficial or to inhibit its growth when it is bad. Other perspectives of our work could be to model the next step that is the reversible attachment which consists of bacterial swarming that is also a very interesting point to look at. All these topics are important to be studied as a further work.

## 5.3 Conclusion

The aim of our work was to model biofilm initiation and bacterial movement toward surfaces. We successfully managed to find the appropriate boundary conditions that describe the phenomenon at the surface. We believe that this work may gain the attention of the experts in biofilms modelling, and may be the motivation for the new ones in this field.

# Bibliography

[1] Wanner, O. and Gujer, W.: A multispecies biofilm model. *Biotechnology and Bioengineering*, vol. 28, no. 3, pp. 314–328, 1986.

[2] Potera, C.: Microbiology: Biofilms invade microbiology. *Science*, vol. 273, no. 5283, pp. 1795–1797, 1996.

[3] Dreeszen, P.H.: Biofilm. *Edstrom*, 2003.

[4] Coghlan, A.: Slime city. *New Scientist*, vol. 151, pp. 32–36, 1996.

[5] Stoodley, H., Luanne, William, C. and Paul, S.: Bacterial biofilms: from the natural environment to infectious diseases. *Review of Microbiology*, vol. 2, pp. 1740–1526, 2004.

[6] Paula, W. and Roberto, K.: Biofilm, city of microbes. *Journal of Bacteriology*, vol. 182, no. 10, pp. 2675–2679, May 2000.

[7] Costerton, J.: Overview of microbial biofilms. *Journal of Industrial Microbiology and Biotechnology*, vol. 15, pp. 137–140, 1995. 10.1007/BF01569816.

[8] Wang, Q. and Zhang, T.: Review of mathematical models for biofilms. *Solid State Communications*, vol. 150, no. 21-22, pp. 1009 – 1022, 2010. Nanoscale Interfacial Phenomena in Complex Fluids.

[9] Niels, H., Thomas, B., Michael, G., Soren, M. and Oana, C.: Antibiotic resistance of bacterial biofilms. *International Journal of Antimicrobial Agents*, vol. 35, pp. 322–332, 2010.

[10] Alfred B. Cunningham, J.E.L. and Ross, R.J.: *Biofilm the hypertextbook, chapter 7, section 2.* 2008.

[11] Tamboto, H.M., Vickery, Karen B.V.Sc., M.P. and Deva, A.K.F.: Subclinical (biofilm) infection causes capsular contracture in a porcine model following augmentation mammaplasty. *Plastic & Reconstructive Surgery*, vol. 126, pp. 835–842, 2010.

[12] Ballyk, M.M., Jones, D.A. and Smith, H.L.: Microbial competition in reactors with wall attachment. *Microbial Ecology*, vol. 41, pp. 210–221, 2001. 10.1007/s002480000005.

[13] Ballyk, M. and Smith, H.: A model of microbial growth in a plug flow reactor with wall attachment. *Mathematical Biosciences*, vol. 158, no. 2, pp. 95 – 126, 1999.

[14] Jones, D., Kojouharov, H.V., Le, D. and Smith, H.: Bacterial wall attachment in a flow reactor. *SIAM Journal*, vol. 62, pp. 1728–1771, 2002.

[15] Kawasaki, K., Mochizuki, A., Matsushita, M., Umeda, T. and Shigesada, N.: Modeling spatio-temporal patterns generated by bacillus subtilis. *Journal of Theoretical Biology*, vol. 188, no. 2, pp. 177 – 185, 1997.

[16] Klapper, I. and Dockery, J.: Mathematical description of microbial biofilms. *SIAM Journal*, vol. 52, no. 2, pp. 221–265, 2010.

[17] Ben Jacob, E., Schochet, O., Tenenbaum, A., Cohen, I., Czirok, A. and Vicsek, T.: Generic modelling of cooperative growth patterns in bacterial colonies. *Nature*, vol. 368, no. 6466, pp. 46–49, March 1994.

[18] Cristian Picioreanu, Mark C. M. van Loosdrecht, J.J.H.: Mathematical modeling of biofilm structure with a hybrid differential-discrete cellular automaton approach. *Biothecnology and Bioengineering,*, vol. 58, 1997.

[19] Poindexter, J.S. and Leadbetter, E.R.: *Bacteria in nature 2: Methods and special applications in bacterial ecology.* Plenum press, New York, 1986.

[20] Jenkinson, H.F. and Lappin-Scott, H.M.: Biofilms adhere to stay. *Trends in Microbiology*, vol. 9, no. 1, pp. 9–10, January 2001.

[21] Costerton, J.W.: Introduction to biofilm. *International Journal of Antimicrobial Agents*, vol. 11, no. 3-4, pp. 217–221, 1999.

[22] Murray, J.D.: *Mathematical Biology I: An Introduction.* Springer, 2002.

[23] Murray, J.D.: *Mathematical Biology II: Spatial Models and Biomedical Applications.* Springer, 2003.

[24] Donnelly, H.: Uniqueness of positive solutions of the heat equation. *American Mathematical Society*, vol. 99, 1987.

[25] Klaus-Jochen Engel, R.N.: *One Parameter Semigroups for linear Evolution Equation.* Springer, 2000.

[26] Goldberg, J.L. and Schwartz, A.J.: *Systems of Ordinary Differential Equations: An Introduction.* Harper and Row.

[27] Jr., D.V.N., Armitage, J.P. and Maini, P.K.: Directional persistence and the optimality of run-and-tumble chemotaxis. *Computational Biology and Chemistry*, vol. 33, no. 4, pp. 269 – 274, 2009.

[28] Keller, E.F. and Segel, L.A.: Model for chemotaxis. *Journal of Theoretical Biology*, vol. 30, no. 2, pp. 225 – 234, 1971.

[29] Tindall, M., Maini, P., Porter, S. and Armitage, J.: Overview of mathematical approaches used to model bacterial chemotaxis ii: Bacterial populations. *Bulletin of Mathematical Biology*, vol. 70, pp. 1570–1607, 2008. 10.1007/s11538-008-9322-5.

[30] Horstmann, D.: From 1970 until present: the keller-segel model in chemotaxis and its consequences. 2003.

[31] Available at: `http://www.mathworks.com/help/techdoc/ref/pdepe.html`

[32] Guyer, J.E., Wheeler, D. and Warren, J.A.: Fipy: Partial differential equations with python. *Computer Science and Engineering*, vol. 11, pp. 6–15, 2009. Available at: `http://www.ctcms.nist.gov/fipy`

[33] Leveque, R.J.: *Finite Volume Methods for Hyperbolic Problems.* Cambridge University Press, 2002.